ACS Pharmacology & Translational Science

pubs.acs.org/ptsci Article

The Influence of Peptide Context on Signaling and Trafficking of Glucagon-like Peptide-1 Receptor Biased Agonists

Zijian Fang,[▽] Shiqian Chen,[▽] Philip Pickford, Johannes Broichhagen, David J. Hodson, Ivan R. Corrêa, Jr., Sunil Kumar, Frederik Görlitz, Chris Dunsby, Paul M. W. French, Guy A. Rutter, Tricia Tan, Stephen R. Bloom, Alejandra Tomas,* and Ben Jones*

Cite This: *ACS Pharmacol. Transl. Sci.* 2020, 3, 345−360 Read Online

ACCESS | Metrics & More | Article Recommendations | Supporting Information

ABSTRACT: Signal bias and membrane trafficking have recently emerged as important considerations in the therapeutic targeting of the glucagon-like peptide-1 receptor (GLP-1R) in type 2 diabetes and obesity. In the present study, we have evaluated a peptide series with varying sequence homology between native GLP-1 and exendin-4, the archetypal ligands on which approved GLP-1R agonists are based. We find notable differences in agonist-mediated cyclic AMP signaling, recruitment of β-arrestins, endocytosis, and recycling, dependent both on the introduction of a His → Phe switch at position 1 and the specific midpeptide helical regions and C-termini of the two agonists. These observations were linked to insulin secretion in a beta cell model and provide insights into how ligand factors influence GLP-1R function at the cellular level.

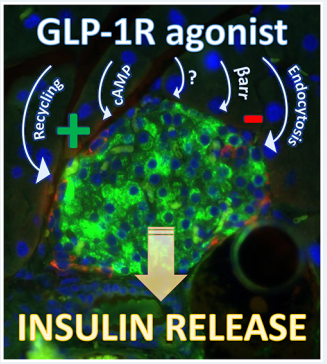

KEYWORDS: *GLP-1R, exendin-4, biased signaling, membrane trafficking, endocytosis, recycling*

Because of the increasing worldwide prevalence of both type 2 diabetes (T2D) and obesity,[1,2] there is considerable interest in the identification and optimization of drugs which can treat both of these conditions. The glucagon-like peptide-1 receptor (GLP-1R) is expressed in pancreatic beta cells and anorectic neurons in the brain, and promotes insulin secretion and weight loss when activated by endogenous or therapeutic peptide ligands.[3] Consequently, GLP-1R agonists (GLP-1RAs) are commonly used to treat T2D and related metabolic diseases.[4]

Activated GLP-1Rs engage with cytosolic G proteins to generate intracellular signaling responses such as production of cyclic adenosine monophosphate (cAMP), elevations in intracellular calcium (Ca^{2+}), and phosphorylation of extracellular regulated kinase (ERK).[5] Concurrent recruitment of β-arrestins terminates G protein signaling but may also facilitate G protein-independent signaling pathways.[6] Ligand-specific signaling pathway preference ("signal bias") has emerged as a factor controlling downstream GLP-1R actions, such as potentiation of insulin secretion,[7] and is of ongoing interest in the therapeutic targeting of other membrane receptors as it provides a potential means to accentuate desirable effects and minimize side effects.[8] Moreover, endocytosis and postendocytic trafficking influence the availability of GLP-1Rs at the cell surface and fine-tune the spatiotemporal origin of signaling responses.[9−11]

The GLP-1 homologue peptide exendin-4 was the first therapeutic GLP-1RA developed for clinical use.[12] Exendin-4 is a high affinity agonist with enhanced resistance to proteolytic degradation in comparison to native GLP-1.[13] Three recent studies indicate how N-terminal amino acid sequence changes to exendin-4 can improve its metabolic effects by generating response profiles that accentuate cAMP generation over β-arrestin recruitment and/or GLP-1R internalization.[14−16] However, it is not known if similar effects can be achieved by modifying the N-terminus of native GLP-1. As the amino acid sequences of a number of approved GLP-1RAs are highly similar to GLP-1 itself, for example, Liraglutide, Dulaglutide, and Semaglutide,[17] this question is of potential therapeutic importance. Furthermore, recent data suggest a potential advantage for GLP-1-like agents over exendin-4-based agonists for clinical outcomes, raising the possibility that the pharmacology of these two agonist subclasses is intrinsically nonidentical.[18,19] A deeper understanding of GLP-1RA structural features that control differential coupling to

Special Issue: Advances in GPCR Signal Transduction

Received: February 24, 2020
Published: March 17, 2020

https://dx.doi.org/10.1021/acsptsci.0c00022
ACS Pharmacol. Transl. Sci. 2020, 3, 345−360

Table 1. Peptides Used in This Study[a]

Peptide	Amino acid sequence
GLP-1	HAEGTFTSDVSSYLQGQAAKQFIAWLVKGR-NH_2
Chimera 1 (Chi1)	HAEGTFTSDVSSYLQGQAAKQFIAWLVKGRPSSGAPPPS-NH_2
Chimera 2 (Chi2)	HAEGTFTSDVSSYLQGQAAKQFIQWLKNGGPSSGAPPPS-NH_2
Chimera 3 (Chi3)	HAEGTFTSDVSSYLQQQAVRLFIQWLKNGGPSSGAPPPS-NH_2
Ex-ala2	HAEGTFTSDLSKQMQQQAVRLFIQWLKNGGPSSGAPPPS-NH_2
Ex4	HGEGTFTSDLSKQMQQQAVRLFIQWLKNGGPSSGAPPPS-NH_2
GLP-1-gly2	HGEGTFTSDVSSYLQGQAAKQFIAWLVKGR-NH_2
GLP-1-phe1	FAEGTFTSDVSSYLQGQAAKQFIAWLVKGR-NH_2
Chi1-phe1	FAEGTFTSDVSSYLQGQAAKQFIAWLVKGRPSSGAPPPS-NH_2
Chi2-phe1	FAEGTFTSDVSSYLQGQAAKQFIQWLKNGGPSSGAPPPS-NH_2
Chi3-phe1	FAEGTFTSDVSSYLQQQAVRLFIQWLKNGGPSSGAPPPS-NH_2
Ex-ala2-phe1	FAEGTFTSDLSKQMQQQAVRLFIQWLKNGGPSSGAPPPS-NH_2
Ex4-phe1	FGEGTFTSDLSKQMQQQAVRLFIQWLKNGGPSSGAPPPS-NH_2
GLP-1-gly2-phe1	FGEGTFTSDVSSYLQGQAAKQFIAWLVKGR-NH_2

[a]The sequences of peptides used in this study in single letter amino acid code. See also Figures S-1A and S-2A.

intracellular effectors and trafficking may aid in the development of better drugs to treat T2D.

In this report we have tested a panel of chimeric peptide GLP-1RAs carrying features of both native GLP-1 and exendin-4, as well as their derivatives modified with a His → Phe switch at position 1. In the context of exendin-4, the latter single amino acid change was previously shown to result in favorable pharmacological characteristics including faster dissociation kinetics, reduced β-arrestin recruitment and endocytosis, faster GLP-1R recycling, and greater insulin secretion *in vitro* and *in vivo*.[15] Here, we use a variety of *in vitro* approaches to demonstrate that peptide-triggered receptor signaling and trafficking properties are influenced by relative homology to GLP-1 versus exendin-4, with introduction of exendin-4-specific midpeptide helical sequences associated with slower GLP-1R recycling and greater desensitization. The effects of the His1 → Phe1 switch are also modulated by contextual sequence differences. These findings highlight the importance of the entire peptide sequence in the development of improved biased ligands targeting GLP-1R.

1. RESULTS

1.1. Peptide Regions Contributing to Binding, Signaling Activity, and Trafficking Responses of Exendin-4 and GLP-1 Chimeric Peptides. We first generated a panel of chimeric peptides bearing features of both GLP-1(7−36)NH_2 (henceforth referred to as "GLP-1") and exendin-4 (Table 1, Supporting Information, Figure S-1A). These were modeled on a series described in an earlier report.[20] In the latter study, the chimeric peptide N-termini were truncated, in order to discern the relative contribution of different structural features to binding affinity; in the present study the N-termini are intact, albeit with amino acid substitutions compared to the parent peptide in some cases. Chimera 1 (Chi1) contains the full sequence of GLP-1 with the addition of the exendin-4 C-terminus; chimera 2 and chimera 3 (Chi2, Chi3) progressively incorporate more of the exendin-4 sequence within the midpeptide helical region. Additionally, to probe the role of the penultimate residues of exendin-4 (Gly) and GLP-1 (Ala), these were switched in two peptides to produce Ex-ala2 and GLP-1-gly2.

Equilibrium binding studies were performed in HEK293 cells expressing N-terminally SNAP-tagged GLP-1R ("HEK293-SNAP-GLP-1R") labeled with the lanthanide time-resolved Förster resonance energy transfer (TR-FRET) donor SNAP-Lumi4-Tb, wherein the binding of unlabeled peptides was measured in competition with the fluorescent ligand exendin-4-FITC.[15] Saturation binding of exendin-4-FITC was determined as part of each experiment (Figure S-1B). The most prominent finding was that the Chi3, Ex-ala2, and exendin-4 peptides showed increased binding affinity compared to GLP-1 itself, while GLP-1-gly2 displayed reduced affinity (Figure 1A, Table 2). Cyclic AMP (cAMP) and β-arrestin-2 recruitment responses were assessed in PathHunter CHO-K1-βarr2-EA-GLP-1R cells (Figure 1B, Table 2). Both Gly2 ligands (exendin-4 and GLP-1-gly2) displayed moderately but consistently reduced efficacy for β-arrestin-2 recruitment, in line with earlier work with exendin-4.[21] However, no ligand showed significant bias toward either pathway when analyzed using the τ/K_A approach derived from the operational model of agonism[22] (Figure 1C).

Because of the important biological role of GLP-1R endocytosis,[9,10,15] we imaged SNAP-GLP-1R endosomal uptake in HEK293 cells via surface SNAP-labeling prior to agonist treatment (Figure 1D). At a single high dose, treatment with all ligands resulted in extensive and similar GLP-1R internalization. We used diffusion-enhanced resonance energy transfer (DERET)[23] to monitor SNAP-GLP-1R internalization in real-time at a range of doses (Figure 1E, Figure S-1C), which confirmed that all ligands were capable of inducing a high level of GLP-1R endocytosis at a maximal dose, albeit with significant differences in potency (Table 3). As postendocytic sorting is an important factor regulating the surface levels of GLP-1R at steady state agonist stimulation,[15] we also measured GLP-1R recycling using a cleavable form of SNAP-Lumi4-Tb ("BG-S-S-Lumi4-Tb"). In this assay, the reducing agent Mesna is used to remove residual GLP-1R labeling at the cell surface after an initial agonist-mediated internalization step, with re-emergence of labeled GLP-1Rs at the cell surface measured in real time after agonist washout through binding to the far red fluorescent GLP-1R antagonist LUXendin645,[24] as previously described using a different acceptor ligand.[25] LUXendin645 showed large and rapid signal increases on binding to Lumi4-Tb-labeled SNAP-GLP-1R (Figure S-1D), indicating its suitability as a TR-FRET acceptor. Using this approach, marked differences in recycling rate versus GLP-1 were observed for GLP-1-gly2 (faster), as well as for Chi2, Chi3, exendin-4, and Ex-ala2, all of which

https://dx.doi.org/10.1021/acsptsci.0c00022
ACS Pharmacol. Transl. Sci. 2020, 3, 345−360

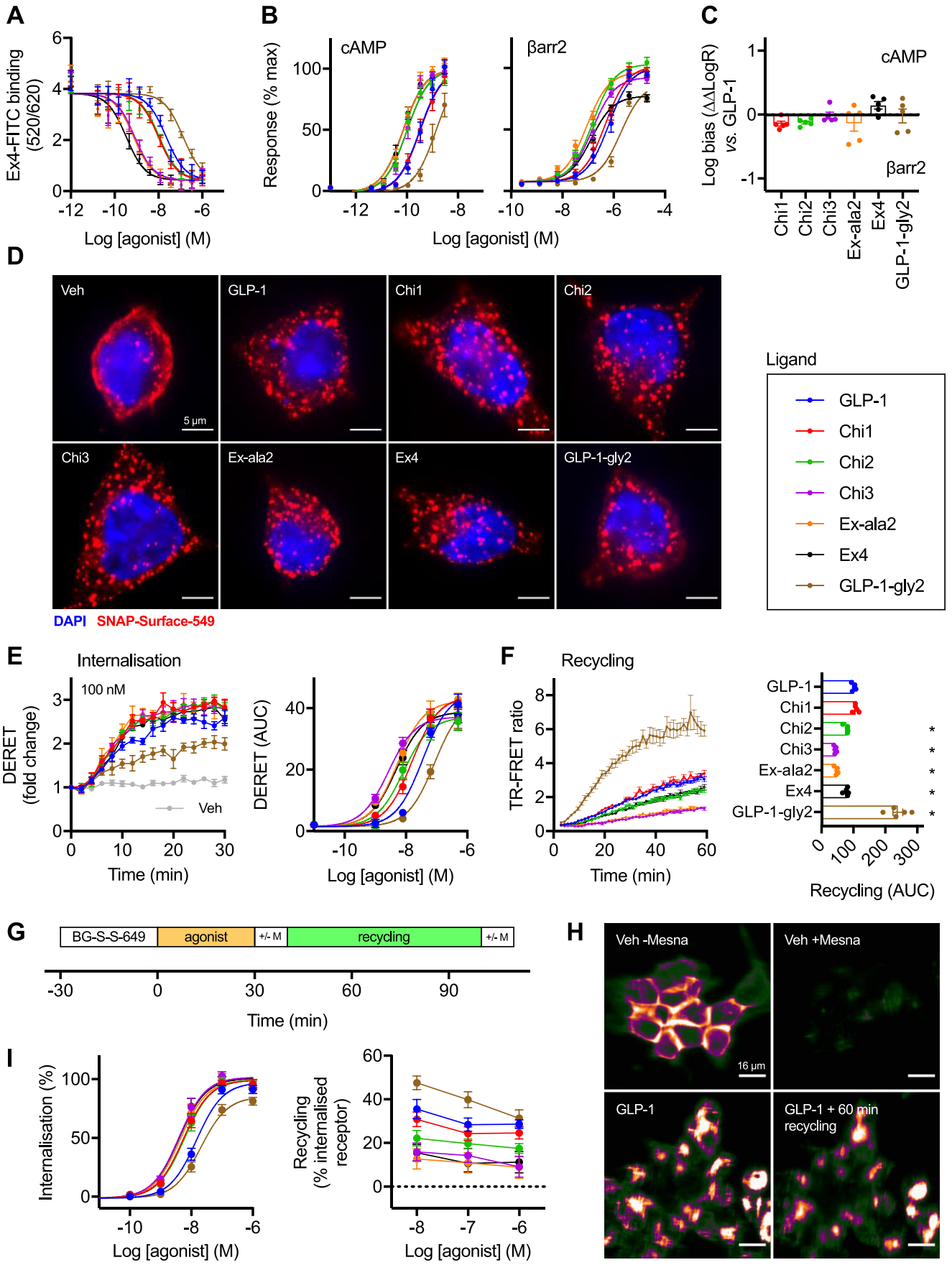

Figure 1. Binding, signaling, and trafficking of chimeric GLP-1R agonist ligands. (A) Equilibrium binding studies in HEK293-SNAP-GLP-1R cells showing TR-FRET-determined binding of 4 nM exendin-4-FITC in competition with indicated concentration of unlabeled agonist, $n = 5$. See also

https://dx.doi.org/10.1021/acsptsci.0c00022
ACS Pharmacol. Transl. Sci. 2020, 3, 345−360

Figure 1. continued

Figure S-1B. (B) cAMP and β-arrestin-2 (βarr2) recruitment responses measured in parallel in CHO-K1-βarr2-EA-GLP-1R cells, n = 5, with 3-parameter fits of pooled data shown. (C) Quantification of signal bias from data presented in (B) using $\Delta\Delta\log \tau/K_A$ method, depicted relative to GLP-1, with statistical comparison performed by one-way randomized block ANOVA with Dunnett's test using $\Delta\log \tau/K_A$ values (i.e., prior to normalization to GLP-1), with no ligand found to be significantly biased relative to GLP-1. (D) Deconvolved widefield microscopy maximum intensity projection images of HEK293-SNAP-GLP-1R cells labeled with SNAP-Surface-549 prior to stimulation with 1 μM agonist for 30 min, representative images of n = 3 independent experiments. Scale bar = 5 μm. (E) Real time SNAP-GLP-1R internalization in HEK293-SNAP-GLP-1R cells, measured by DERET, with response to 100 nM agonist shown as well as concentration responses representing AUC from traces shown in Figure S-1C, n = 5, with 3-parameter fits of pooled data. (F) SNAP-GLP-1R recycling measured by TR-FRET in CHO-K1-SNAP-GLP-1R cells after BG-S-S-Lumi4-Tb labeling, stimulation with 100 nM agonist for 30 min, cleavage of residual surface BG-S-S-Lumi4-Tb, and 60 min recycling in the presence of LUXendin645 (10 nM), n = 5, with AUC compared by one-way randomized block ANOVA with Dunnett's test versus GLP-1. (G) Principle of high content microscopy assay to measure GLP-1R internalization and recycling. (H) Example images taken from high content microscopy assay, showing the effect of Mesna on vehicle-treated cells (to demonstrate the efficiency of surface cleavage of BG-S-S-649) and of cells treated with 1 μM GLP-1 and then sequential Mesna application before and after recycling period (demonstrating signal intensity reduction from the same cell population reflecting cleavage of recycled surface receptor), scale bar = 16 μm. (I) Internalization and recycling responses of chimeric GLP-1R ligands measured in HEK293-SNAP-GLP-1R cells by high content microscopy, 3-parameter fits of pooled internalization data shown, n = 11 for internalization and n = 5 for recycling. Data represented as mean ± SEM, with individual replicates shown in some cases.

Table 2. Binding and Signalling Parameter Estimates for Chimeric Peptides[a]

	Equilibrium binding	cAMP			β-arrestin-2		
	pK_i (M)	pEC_{50} (M)	E_{max} (%)	log τ/K_A (M)	pEC_{50} (M)	E_{max} (%)	log τ/K_A (M)
GLP-1	7.8 ± 0.1	9.5 ± 0.1	100	9.5 ± 0.1	6.2 ± 0.1	102 ± 5	6.2 ± 0.1
Chi1	8.2 ± 0.2	9.5 ± 0.1	100	9.5 ± 0.1	6.4 ± 0.1	102 ± 6	6.4 ± 0.1
Chi2	8.2 ± 0.1*	10.0 ± 0.1*	100	10.0 ± 0.1*	6.9 ± 0.1*	104 ± 6	6.9 ± 0.1*
Chi3	9.4 ± 0.1*	10.0 ± 0.1*	100	10.0 ± 0.1*	6.9 ± 0.2*	93 ± 5*	6.8 ± 0.1*
Ex4-ala2	9.4 ± 0.1*	10.1 ± 0.1*	100	10.1 ± 0.1*	7.1 ± 0.2*	97 ± 5	6.8 ± 0.1*
Ex4	9.7 ± 0.1*	10.2 ± 0.1*	100	10.1 ± 0.1*	6.9 ± 0.1*	77 ± 3*	7.0 ± 0.1*
GLP-1-gly2	7.1 ± 0.1*	8.8 ± 0.1*	100	8.9 ± 0.1*	5.7 ± 0.1*	87 ± 4*	5.7 ± 0.1*

[a]Mean ± SEM parameter estimates from data shown in Figure 1, n = 5 experimental repeats. Binding experiments were performed in HEK293-SNAP-GLP-1R cells, signaling experiments were performed in CHO-K1-βarr2-EA-GLP-1R cells. Signaling parameter estimates were determined from 3-parameter fitting. E_{max} values are expressed relative to the global maximum for full agonists in each assay; note that all compounds are full agonists for cAMP in this cell model, so E_{max} was globally constrained to 100% in that assay. *$p < 0.05$ versus GLP-1, determined by one-way ANOVA with Dunnett's test.

Table 3. GLP-1R Internalization Concentration Response Parameter Estimates for Chimeric Ligands in HEK293-SNAP-GLP-1R Cells[a]

	DERET			High Content Microscopy Assay		
	pEC_{50} (M)	E_{max} (AUC)	log τ/K_A (M)	pEC_{50} (M)	E_{max} (% internalization)	log τ/K_A (M)
GLP-1	7.5 ± 0.1	46 ± 3	7.6 ± 0.1	7.8 ± 0.1	98 ± 3	7.8 ± 0.1
Chi1	7.8 ± 0.1	45 ± 1	7.8 ± 0.1	8.2 ± 0.1*	100 ± 3	8.2 ± 0.1*
Chi2	8.1 ± 0.1*	38 ± 4	8.0 ± 0.1*	8.2 ± 0.1*	101 ± 3	8.2 ± 0.1*
Chi3	8.5 ± 0.1*	38 ± 2	8.4 ± 0.1*	8.4 ± 0.1*	103 ± 4	8.4 ± 0.1*
Ex4-ala2	8.3 ± 0.1*	43 ± 2	8.5 ± 0.1*	8.3 ± 0.1*	101 ± 5	8.3 ± 0.1*
Ex4	8.2 ± 0.0*	39 ± 2	8.3 ± 0.1*	8.4 ± 0.1*	92 ± 3	8.4 ± 0.1*
GLP-1-gly2	7.0 ± 0.2	45 ± 5	7.1 ± 0.1	7.7 ± 0.1*	86 ± 3*	7.8 ± 0.1

[a]Mean ± SEM signaling parameter estimates from concentration response data shown in Figure 1, i.e., DERET assay (Figure 1E), n = 5, and high content microscopy assay using BG-S-S-649 (Figure 1I), n = 11. Signaling parameter estimates were determined from 3-parameter fitting. *$p < 0.05$ versus GLP-1, determined by one-way ANOVA with Dunnett's test.

recycled more slowly than GLP-1 itself (Figure 1F). These findings were confirmed by microscopy (Figure S-1E).

We also developed a high-content microscopy assay to sequentially measure GLP-1R internalization and recycling at multiple doses using the Mesna-cleavable SNAP-tag probe BG-S-S-649 (Figure 1G). This assay represents a higher throughput adaption of an earlier flow cytometry assay.[10] The far red DY-649 fluorophore was considered particularly suitable as it avoids the higher autofluorescence of plastic microplates at lower wavelengths. Sequential applications of Mesna after internalization and recycling allowed determination of receptor distribution from the same fields of view within each well. Example images showing the effect of Mesna application before and after recycling are shown in Figure 1H (note that quantification was performed from several fields-of-view per well, representing many hundreds of cells). Results were broadly consistent with those obtained with the TR-FRET based assays (Figure 1I, Table 3).

https://dx.doi.org/10.1021/acsptsci.0c00022
ACS Pharmacol. Transl. Sci. 2020, 3, 345−360

Table 4. Binding and Signalling Parameter Estimates for His1- and Phe1-Containing Chimeric Ligands[a]

	Equilibrium binding	cAMP			β-arrestin-2		
	pK_i (M)	pEC_{50} (M)	E_{max} (%)	log τ/K_A (M)	pEC_{50} (M)	E_{max} (%)	log τ/K_A (M)
GLP-1	8.5 ± 0.1	9.4 ± 0.1	100	9.3 ± 0.1	6.4 ± 0.2	111 ± 7	6.4 ± 0.1
GLP-1-phe1	6.9 ± 0.1*,#	8.1 ± 0.2*,#	100	8.1 ± 0.1*,#	5.7 ± 0.1*,#	61 ± 7*,#	5.4 ± 0.1*,#
Chi1	8.6 ± 0.1	9.5 ± 0.1	100	9.5 ± 0.1	6.6 ± 0.1	108 ± 6	6.6 ± 0.1
Chi1-phe1	6.9 ± 0.1*,#	8.1 ± 0.2*,#	100	8.1 ± 0.2*,#	5.6 ± 0.0*,#	55 ± 7*,#	5.2 ± 0.1*,#
Chi2	8.7 ± 0.2	10.0 ± 0.1*	100	9.9 ± 0.1*	7.0 ± 0.1*	108 ± 6	7.0 ± 0.1*
Chi2-phe1	6.4 ± 0.1*,#	8.8 ± 0.2*,#	100	8.7 ± 0.2*,#	5.9 ± 0.0*,#	62 ± 5*,#	5.5 ± 0.1*,#
Chi3	9.5 ± 0.1*	9.9 ± 0.1*	100	9.8 ± 0.1*	7.0 ± 0.1*	105 ± 7	7.0 ± 0.1
Chi3-phe1	8.3 ± 0.1#	9.4 ± 0.2#	100	9.3 ± 0.2#	6.3 ± 0.1#	53 ± 5*,#	5.9 ± 0.1 #
Ex-ala2	9.8 ± 0.1*	10.0 ± 0.1*	100	10.0 ± 0.1*	7.3 ± 0.1*	105 ± 8	7.2 ± 0.1*
Ex-ala2-phe1	8.4 ± 0.1#	9.8 ± 0.1*	100	9.8 ± 0.1*	6.7 ± 0.1#	51 ± 5*,#	6.2 ± 0.0 #
Ex4	9.9 ± 0.1*	10.0 ± 0.1*	100	10.1 ± 0.1*	7.2 ± 0.1*	87 ± 4	7.0 ± 0.1
Ex-phe1	7.8 ± 0.1*,#	9.0 ± 0.2*,#	100	8.9 ± 0.2*,#	6.0 ± 0.2 #	12 ± 1*,#	4.6 ± 0.2*,#
GLP-1-gly2	7.2 ± 0.1*	8.8 ± 0.1*	100	8.8 ± 0.1*	5.8 ± 0.0*	101 ± 5	5.8 ± 0.0*
GLP-1-gly2-phe1	6.5 ± 0.2*,#	7.0 ± 0.2*,#	100	7.1 ± 0.2*,#	4.8 ± 0.2*,#	16 ± 1*,#	3.6 ± 0.3*,#

[a]Mean ± SEM signaling parameter estimates from data shown in Figure 2 and Figure S-2, $n = 5$ experimental repeats. Binding experiments were performed in HEK293-SNAP-GLP-1R cells, signaling experiments were performed in CHO-K1-βarr2-EA-GLP-1R cells. Signaling parameter estimates were determined from 3-parameter fitting. E_{max} values are expressed relative to the global maximum for full agonists in each assay. All compounds are full agonists for cAMP in this assay, so E_{max} was globally constrained to 100%. *$p < 0.05$ versus GLP-1, and #$p < 0.05$ for Phe1 ligand versus corresponding His1 ligand, determined by one-way ANOVA with Tukey's test.

Finally, coupling of occupancy to cAMP signaling, β-arrestin-2 recruitment and endocytosis was compared by subtracting log τ/K_A estimates from affinity measures and normalizing to GLP-1 as the reference ligand (Figure S-1F). This analysis showed that the highest affinity ligands Chi3, Ex-ala2, and exendin-4 were less well coupled to functional responses than GLP-1, that is, the greater affinity of these ligands did not result in commensurate increases in signaling.

These results highlight how sequence divergence between GLP-1 and exendin-4 can influence the binding affinity, signaling potency, and trafficking characteristics of GLP-1R agonist ligands.

1.2. N-Terminal Substitution Differentially Affects Binding, Signaling, and Trafficking Characteristics of Chimeric Peptides. Substitution of the exendin-4 N-terminal His to Phe results in reduced β-arrestin recruitment and internalization.[15] Nevertheless, structural differences in the host peptide might lead to changes to agonist orientation, N-terminal flexibility, and receptor interactions formed by agonist residues in the immediate vicinity, modulating the effects of the Phe1 substitution. We pharmacologically evaluated Phe1 analogues (Table 1, Figure S-2A) of the chimeric peptide series, first measuring binding affinities at equilibrium in HEK-SNAP-GLP-1R cells (Figure S-2B, Table 4). All Phe1 ligands showed reduced affinity compared to their His1 counterparts, included in the assay for parallel comparisons. Cyclic AMP signaling and β-arrestin-2 recruitment responses for each ligand were assessed in CHO-K1-βarr2-EA-GLP-1R cells (Figure 2A, Table 4). The most notable finding was a significantly reduced efficacy for β-arrestin-2 recruitment for all Phe1 ligands, particularly when Phe1 was introduced to both exendin-4 and GLP-1-gly2, with a more moderate effect for ligands containing Ala2 instead of Gly2. Coupling selectivity of each ligand relative to GLP-1 is displayed in the heatmap, demonstrating that Phe1 analogues incorporating more of the exendin-4 sequence show progressively greater bias toward cAMP signaling, with Ex-phe1 being the most prominent example. Bias estimates are also displayed in an alternative format in Figure S-2C. Coupling of the occupancy to cAMP signaling and β-arrestin-2 recruitment was determined from the subtraction of log τ/K_A estimates for each pathway from pK_i for each ligand (Figure S-2D). This analysis suggests that introduction of Phe1 to Chi2, Chi3, Ex-ala2, and exendin-4 results in improved coupling to cAMP production, with lesser effects on β-arrestin-2 recruitment.

To gain further insights into signaling differences between His1 and Phe1 ligands, we used NanoBiT complementation[26] to measure recruitment of both catalytically inactive mini-G_s protein[27] and β-arrestin-2 to GLP-1R. Here, complementary elements of the 19.1 kDa nanoluciferase enzyme have been appended to the GLP-1R C-terminus and the mini-G_s N-terminus or β-arrestin-2 C-terminus, allowing monitoring of dynamic changes in G_s protein and β-arrestin-2 recruitment. A high ligand concentration (1 μM) was specifically chosen to ensure a high degree of receptor occupancy (at least 70% for the lowest affinity agonist Chi2-Phe1 according to the law of mass action[28]) in order to provide efficacy data without requiring full concentration responses. Here, all Phe1 ligands demonstrated reduced efficacy compared to His1 equiv for both mini-G_s (Figure 2B, Figure S-2E) and β-arrestin-2 recruitment (Figure 2C, Figure S-2F). GLP-1R internalization was also measured by DERET, with all Phe1 ligands displaying severely reduced endocytic tendency (Figure 2D, Figure S-2G). Phe1 ligands also recycled faster than their His1 equiv in all cases, as detected using TR-FRET (Figure 2E, Figure S-2H), except for GLP-1-gly2-phe1, for which the His1 version also shows rapid recycling. High content microscopy showed a similar pattern in both internalization and recycling (Figure S-2I, J).

To allow comparison of ligand characteristics, responses for each assay are compared in the heatmap shown in Figure 2F after normalization to the most efficacious ligand on a per-assay basis. This highlights how the Phe1 group of ligands show lower efficacy for each of the recruitment and internalization readouts. The most dramatic impact is observed within (Gly2-containing) exendin-4 and GLP-1-gly2, in keeping with a similar finding for β-arrestin-2 efficacy using the PathHunter system (Figure 2A), and confirmed by

https://dx.doi.org/10.1021/acsptsci.0c00022
ACS Pharmacol. Transl. Sci. 2020, 3, 345−360

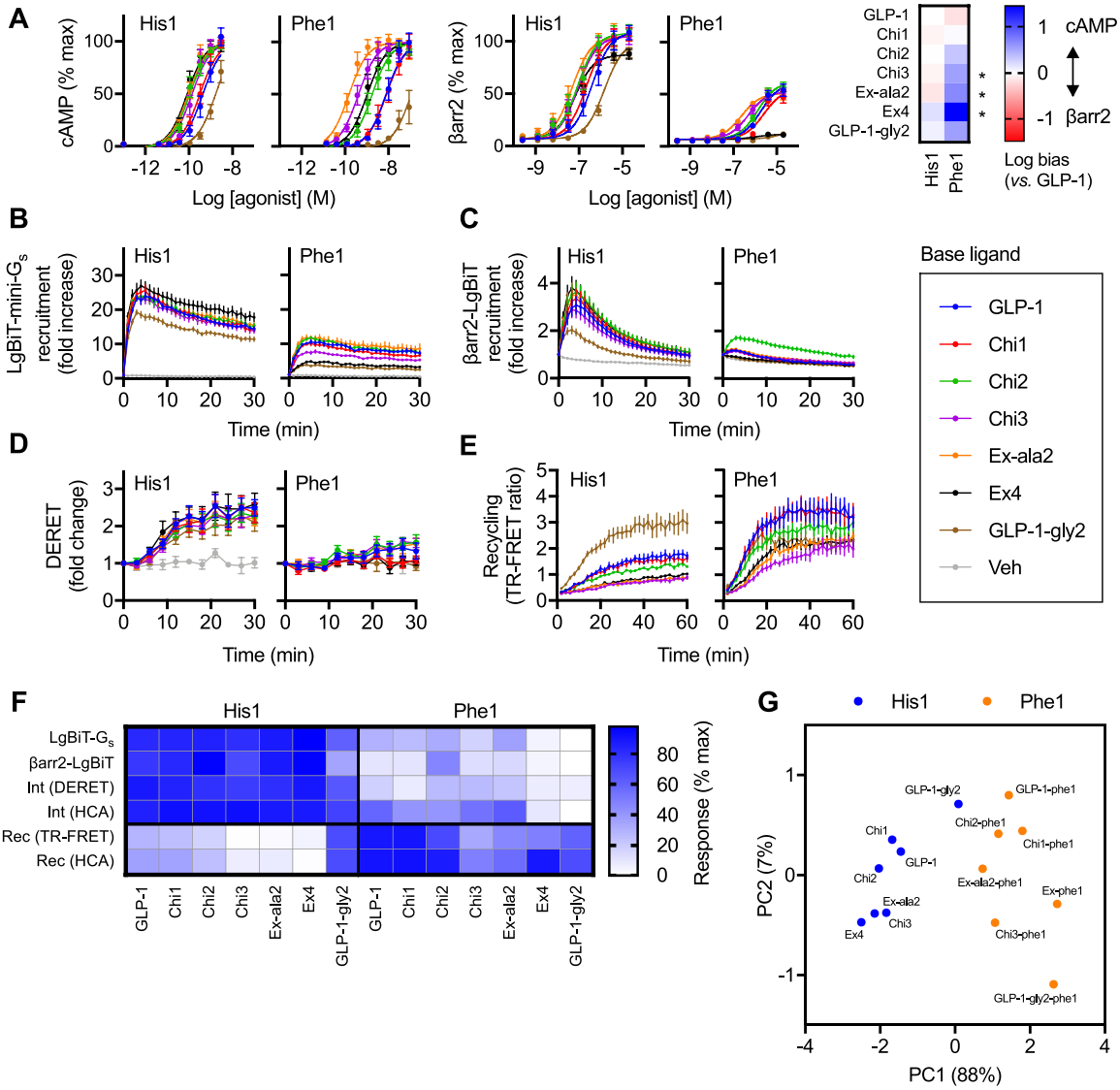

Figure 2. Pharmacological characterization of N-terminally substituted chimeric GLP-1R agonists. (A) cAMP and β-arrestin-2 recruitment responses in CHO-K1-βarr2-EA-GLP-1R cells, n = 5, with 3-parameter fits of pooled data shown; the heatmap shows signal bias quantified using the $\Delta\Delta\log \tau/K_A$ method bias relative to GLP-1; statistical comparison was performed by one-way randomized block ANOVA with Sidak's test to compare bias for each His1/Phe1 ligand pair using $\Delta\log \tau/K_A$ values (i.e., prior to normalization to GLP-1). (B) NanoBiT measurement of LgBiT-mini-G_s recruitment to GLP-1R-SmBiT in HEK293T cells after stimulation with a saturating (1 μM) concentration of ligand, n = 5. (C) As for panel B, but for βarr2-LgBit. (D) As for panel B, but for GLP-1R internalization in HEK293-SNAP-GLP-1R cells measured by DERET. (E) SNAP-GLP-1R recycling measured by TR-FRET in CHO-K1-SNAP-GLP-1R cells after BG-S-S-Lumi4-Tb labeling, stimulation with 1 μM agonist for 30 min, cleavage of residual surface BG-S-S-Lumi4-Tb, and 60 min recycling in the presence of LUXendin645 (10 nM), n = 5. (F) Representation of data shown in panels B–E, Figures S-2I and S-2J (internalization ["Int"] and recycling [Rec] measured by high content microscopy analysis [HCA]), showing the mean response of each ligand with normalization to the minimum and maximum ligand response in each assay repeat. (G) Principal component analysis of His1 and Phe1 ligands, derived from single dose response data from panels B and C, and Figures S-2I and S-2J. *p < 0.05 by statistical test indicated in the text. Data represented as mean ± SEM.

expressing the response of each Phe1 agonist as a percentage of that of its His1 counterpart (Figure S-2K). Recycling typically displayed the inverse pattern, although more overlap was observed between the Phe1 and His1 groups, for example, the Chi3-phe1 and Ex-ala2-phe1-induced recycling rates approached those of the slower His1 ligands. Further analysis revealed a relationship between GLP-1R binding affinity and recycling rate, which was most apparent for agonists with moderate affinity (Figure S-2L). Principal component analysis[29] was used to visually represent the clustering of agonists showing similar signaling and trafficking characteristics (Figure 2G). Phe1 were clearly distinguished from His1 ligands within the first principal component (PC1, accounting for 88% of the total variance). Of note, the exendin-4/Ex-phe1 pairs were separated to the greatest degree within PC1.

These results highlight how the Phe1 substitution can markedly affect the pharmacology of GLP-1R ligands, but to varying degrees dependent on other ligand sequence features.

1.3. Effect of Chimeric GLP-1RA Peptides in Beta Cells. Cellular context can influence the manifestations of signal bias.[30] A major site of action for native GLP-1 and its therapeutic mimetics is the pancreatic beta cell, where it is coupled to potentiation of insulin secretion.[7] We therefore performed further assessments of His1 and Phe1 peptides in

https://dx.doi.org/10.1021/acsptsci.0c00022
ACS Pharmacol. Transl. Sci. 2020, 3, 345−360

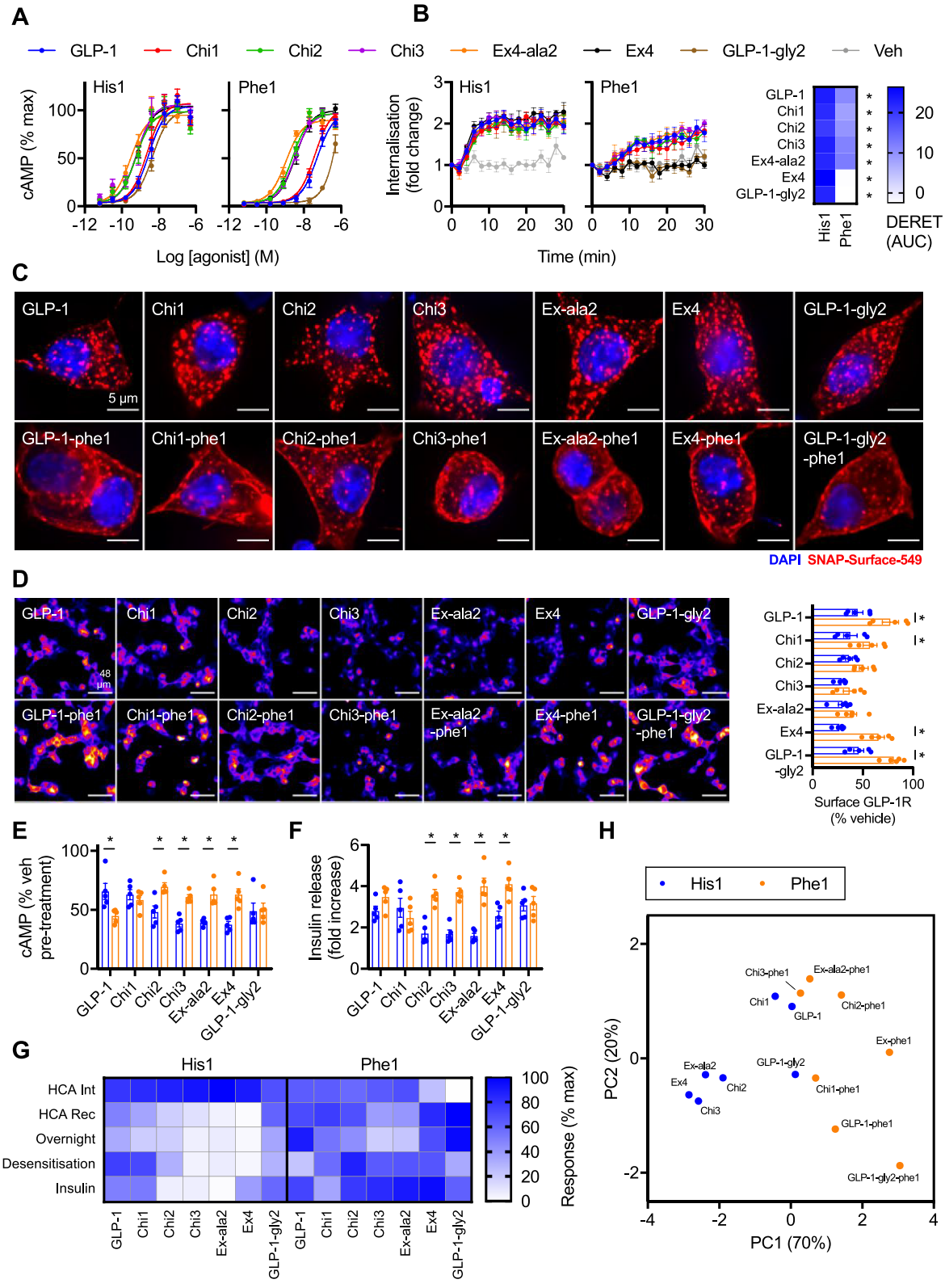

Figure 3. Effects of biased chimeric peptides in beta cells. (A) cAMP responses in INS-1 832/3 cells with endogenous GLP-1R expression stimulated for 10 min in the presence of 500 μM IBMX, n = 5. (B) GLP-1R internalization measured by DERET in INS-1-SNAP-GLP-1R cells stimulated with 1 μM agonist, n = 5, with quantification of AUC shown on the heatmap and statistically compared by one-way randomized block ANOVA with Sidak's test for each His1 versus Phe1 ligand pair. (C) Widefield microscopy images of INS-1-SNAP-GLP-1R cells labeled with SNAP-Surface-549 prior to stimulation with 1 μM agonist for 30 min, representative images of n = 3 independent experiments. Scale bar = 5 μm. (D) Representative images showing GLP-1R surface expression levels detected by SNAP-Surface-649 labeling performed after 16-h exposure to 1 μM agonist, scale bar = 48 μm, with quantification of n = 5 experiments and comparison by one-way randomized block ANOVA with Sidak's test for each His1 versus Phe1 ligand pair. (E) Homologous desensitization experiment in wild-type INS-1 832/3 treated for 16 h with 1 μM agonist, followed by washout, 1-h recovery, and rechallenged with 100 nM GLP-1 + 500 μM IBMX, normalized to response to vehicle pretreated cells, n =

https://dx.doi.org/10.1021/acsptsci.0c00022
ACS Pharmacol. Transl. Sci. 2020, 3, 345−360

Figure 3. continued

5, one-way randomized block ANOVA with Sidak's test for each His1 versus Phe1 ligand pair. (F) Insulin secretion from wild-type INS-1 832/3 cells treated with 11 mM glucose ± 1 μM agonist for 16 h, expressed relative to vehicle, $n = 5$, one-way randomized block ANOVA with Sidak's test for each His1 versus Phe1 ligand pair. (G) Representation of data shown in Figures S-3B and S-3D, and panels D−F, showing the mean response of each ligand with normalization to the minimum and maximum ligand response in each assay repeat. (H) Principal component analysis of His1 and Phe1 ligands, derived from single dose response data from as represented in panel G. *$p < 0.05$ by statistical test indicated in the text. Data represented as mean ± SEM, with individual replicates shown in some cases.

INS-1 832/3 cells,[31] a clonal beta cell line of rat origin. cAMP signaling responses were consistent with the patterns observed in CHO-K1-βarr2-EA-GLP-1R cells, with reduced potency observed with all Phe1 versus equivalent His1 ligands (Figure 3A, Figure S-3A, Table 5). SNAP-GLP-1R endocytosis

Table 5. cAMP Signalling Parameter Estimates of His1- and Phe1-Containing Chimeric Ligands in INS-1 832/3 Cells[a]

	pEC_{50} (M)	E_{max} (%)
GLP-1	8.6 ± 0.2	100
GLP-1-phe1	7.3 ± 0.1*,#	100
Chi1	8.7 ± 0.2	100
Chi1-phe1	7.5 ± 0.1*,#	100
Chi2	9.2 ± 0.2*	100
Chi2-phe1	8.6 ± 0.1#	100
Chi3	9.3 ± 0.2*	100
Chi3-phe1	8.4 ± 0.1#	100
Ex-ala2	9.4 ± 0.2*	100
Ex-ala2-phe1	8.8 ± 0.1#	100
Ex4	9.3 ± 0.2*	100
Ex-phe1	8.4 ± 0.2#	100
GLP-1-gly2	8.3 ± 0.1	100
GLP-1-gly2-phe1	6.4 ± 0.1*,#	100

[a]Mean ± SEM signaling parameter estimates from data shown in Figure 3, $n = 5$ experimental repeats. Signaling parameter estimates were determined from 3-parameter fitting. All compounds are full agonists for cAMP in this cell model, so E_{max} was globally constrained to 100%. *$p < 0.05$ versus GLP-1, and #$p < 0.05$ for Phe1 ligand versus corresponding His1 ligand, determined by one-way ANOVA with Tukey's test.

following treatment with each agonist was monitored in INS-1 832/3 cells by DERET (Figure 3B, Figure S-3B) and confirmed by microscopy (Figure 3C). All Phe1 ligands led to less internalization, with Gly2-containing Ex-phe1 and GLP-1-gly2-phe1 showing virtually undetectable DERET responses. The DERET assay also showed approximately twice as fast GLP-1R uptake in INS-1 832/3 compared to HEK293-SNAP-GLP-1R cells (i.e., Figure 2D), and that the Phe1 ligand responses in the beta cell model (except for Ex-phe1 and GLP-1-gly2-phe1) were less diminished compared with the equivalent His1 ligand response (see Table S-1 for kinetic comparisons). High content microscopy also showed reduced internalization with Phe1 ligands, especially for Ex-phe1 and GLP-1-gly2-phe1 (Figure S-3C), and further highlighted how Phe1 agonist-mediated GLP-1R internalization was less reduced in the beta cell model (Figure S-3D). Phe1 ligands recycled faster than His1 equiv (Figure S-3E), with higher affinity Chi3-phe1 and Ex-ala2-phe1 showing the slowest recycling rates among the Phe1 ligands.

As the functional effects of biased GLP-1R ligands such as Ex-phe1 tend to emerge after prolonged stimulations,[15] we tested the effect of a 16-h exposure to each ligand on beta cell GLP-1R distribution by surface SNAP-labeling at the end of the exposure period. Note that this approach detects both recycled and newly synthesized GLP-1Rs, unlike the recycling assays used earlier in the present study in which only the receptor labeled prior to stimulation is measured. Nevertheless, results were generally consistent with the trafficking characteristics of each ligand, with Phe1 agonists preserving more surface GLP-1R at the end of the exposure period than His1 agonists, with the exception of the Chi3/Chi3-phe1 and Ex-ala2/Ex-ala2-phe1 pairs (Figure 3D). To test the functional implications of these trafficking differences, we assessed for homologous GLP-1R desensitization with each ligand by pretreating for 16 h, washing, and allowing a 1-h recycling period before rechallenging with a fixed dose of GLP-1. Here, prior treatment with the slow recycling, high affinity His1 ligands Chi2, Chi3, Ex-ala2, and exendin-4 led to greater desensitization, whereas the equivalent Phe1 analogues allowed cells to retain more responsiveness (Figure 3E). Similarly, continuous exposure to the same set of Phe1 ligands led to higher levels of cumulative insulin secretion (Figure 3F), suggesting that sustained insulinotropism is partly controlled by GLP-1R trafficking. To check that these findings were not artifacts of differences in potency, we also measured sustained insulin secretion with GLP-1, GLP-1-phe1, exendin-4, and Ex-phe1 over a range of doses, comparing these findings with previously determined acute cAMP potency measurements (Figure S-3F,G). This indicated that both GLP-1-like ligands displayed a relative reduction in potency for sustained insulin secretion versus acute cAMP potency compared to the exendin peptides, likely to indicate accelerated ligand degradation, but also that the high ligand dose used in earlier experiments remained maximal during prolonged exposure (and is therefore indicative of efficacy).

Thus, Phe1 ligands were generally characterized by slower internalization, faster recycling, reduced net loss of surface GLP-1R and desensitization, as well as greater cumulative insulin secretion. However, comparison of the relative responses of each ligand in each assay indicated that trafficking characteristics did not entirely predict functional responses (Figure 3G). For example, within the Phe1 group of ligands, Chi3-phe1 and Ex-ala2-phe1 showed the greatest loss of surface receptor after overnight exposure, in keeping with their somewhat greater acute internalization and reduced recycling; however, this was not associated with commensurate increases in desensitization or reduced insulin secretion. Nevertheless, principal component analysis incorporating functional cAMP and insulin readouts as well as trafficking data again showed clear discrimination of Phe1 versus His1 peptides, with Ex-phe1 and exendin-4 showing the most marked difference within the first principal component (Figure 3H). A correlation matrix summarizing the relationship between agonist parameters measured across the different cell lines used in this study is shown in Figure S-3H.

Thus, the overall pattern of biased GLP-1R action identified in HEK293 and CHO-K1 cells was at least partially replicated

https://dx.doi.org/10.1021/acsptsci.0c00022
ACS Pharmacol. Transl. Sci. 2020, 3, 345−360

in a beta cell model. The functional impact of altered GLP-1R trafficking partly, but not entirely, explained the differences in sustained insulin secretion observed with the Phe1 ligands.

2. DISCUSSION

In this study we evaluated a series of GLP-1R ligands with variable sequence homology to GLP-1 and exendin-4, focusing in particular on their effects on signal bias and GLP-1R trafficking. We previously found that the functional and therapeutic effects of exendin-4-derived peptides can be profoundly affected by N-terminal sequence modifications that preferentially alter β-arrestin recruitment, GLP-1R endocytosis and recycling.[15] The present work builds on our earlier findings by assessing further ligand factors that influence these processes.

We developed a high content microscopy-based assay to measure GLP-1R internalization and recycling in the same assay using a cleavable SNAP-tag-labeling far red fluorescent probe. This approach was adapted from earlier work by us[10] and others[32] in which similar fluorescent probes were used in lower throughput assays based on flow cytometry and confocal microscopy, respectively. Simultaneous handling of multiple ligands or ligand doses in multiwell plates, along with data acquisition from several fields of view at relatively lower magnification, enhances experimental reproducibility and statistical robustness compared to lower throughput methods.[33] The cleavable BG-S-S-Lumi4-Tb TR-FRET method for measuring GLP-1R recycling provided generally concordant results with those obtained using the high content assay. One example where results did not entirely agree was for exendin-4 versus Ex-phe1 (Figure 2F), but it is not clear if this represents experimental variability, cell-type differences (HEK293 versus CHO-K1), or methodological variances, for example, due to the more indirect method of detection with the TR-FRET assay. The latter method gives additional kinetic information not available from our implementation of the microscopy-based Mesna cleavage method, although fast-recycling events could in principle be studied by monitoring fluorescence loss in real time during continuous Mesna exposure.[32] This was not attempted here as, for many of the slow-recycling ligands, the required exposure time to a reducing environment and nonphysiological pH would lead to nonspecific effects on cell behavior.

We found clear binding, signaling, and internalization differences between GLP-1 and exendin-4, with affinity for the latter being approximately 5 times greater and potency (for most readouts) approximately 10 times greater. As the GLP-1 amino acid sequence was progressively replaced by that of exendin-4, starting at the C-terminus, both affinity and potency increased. Of note, the impact of adding the exendin-4 C-terminal extension, or "Trp-cage", was small, consistent with other studies in which its truncation had little effect on exendin-4 signaling.[34] It should be noted that, once occupancy differences are taken into account, exendin-4-like ligands show a comparative signaling deficit, as greater affinity did not fully translate into commensurate increases in signaling potency. A recent report describes the detection of two separate binding sites for exendin-4 on the GLP-1R extracellular domain (ECD), potentially in keeping with previous photoaffinity cross-linking data[35] and apparently responsible for impaired receptor oligomerization compared to nonexendin-4 ligands.[36] As GLP-1R dimerization is required for full signaling efficacy,[37] it is possible that this phenomenon partly explains our results. However, the full-length GLP-1R may not behave identically to the isolated ECD.[38,39] The Ala → Gly switch at position 2, seen in exendin-4 and GLP-1-gly2, was noted in the present study to modestly reduce recruitment efficacy for β-arrestin-2 in both cases. This is in keeping with previous work[21] and potentially relevant to the signaling characteristics of Phe1 ligands (see below). Contrasting with this consistent signaling efficacy effect, the affinity of GLP-1-gly2 was almost 10-fold reduced versus GLP-1, whereas exendin-4 showed similar binding characteristics to Ex-ala2. This highlights how binding affinity of GLP-1-like peptides depends more on interactions with the receptor core made by their N-terminal regions than for exendin-4-like ligands, for which the more helical midpeptide regions and C-terminus allow stable interactions with the ECD.[20]

None of the His1-containing ligands showed significant bias between cAMP generation or -arrestin-2 recruitment relative to GLP-1, although a trend for cAMP-preference was observed for exendin-4, in keeping with some[21] but not all[11] previous literature. Moreover, endocytosis potency differences generally followed the pattern established for cAMP and β-arrestin-2 signaling. GLP-1R recycling measured by two different methods highlighted clear differences in GLP-1-like versus exendin-4-like peptides across a wide range of doses, with the latter showing more gradual recycling. A similar pattern was found for GLP-1 versus exendin-4 in a previous study.[40] In the latter work, the difference was suggested to be partly related to GLP-1 degradation by dipeptidyl dipeptidase-4 (DPP-4), which cleaves at the penultimate Ala residue close to the N-terminus and to which exendin-4 is resistant by virtue of the Ala → Gly switch at position 2. However, our observation of slow recycling with DPP-4-sensitive Ex-ala2 suggests that DPP-4 is unlikely to be a critical determinant of GLP-1R recycling. Interestingly, endothelin converting enzyme-1 (ECE-1) has recently been shown to play a role in the control of GLP-1R recycling and desensitization,[41] presumably due to intra-endosomal ligand degradation and subsequent rerouting of unbound GLP-1R to a recycling pathway. Because of its enhanced resistance to other endopeptidases such as neprilysin,[42] exendin-4 is likely to be ECE-1-resistant, although this has not been confirmed experimentally. In conjunction with its higher binding affinity, this could potentially contribute to more persistent intraendosomal GLP-1R occupancy, resulting in accentuated targeting to postendocytic degradative pathways. This possibility could be amenable to future exploration.

Because of the beneficial effects of exendin-phe1,[15] we wished to determine whether sequence changes elsewhere in the peptide would modulate the effects of the Phe1 N-terminal substitution. Concentration response experiments in CHO-K1 cells revealed reduced efficacy for β-arrestin-2 with Phe1 ligands in all cases, although the effect was most apparent with the Gly2-containing Ex-phe1 and GLP-1-gly2-phe1, for which β-arrestin-2 recruitment was virtually undetectable, even in the inherently amplified DiscoverX system. The efficacy reduction for the combination of Phe1 and Gly2 appeared to be at least additive. Interestingly, pathway bias analysis did not universally show that this reduction in β-arrestin-2 efficacy translated to significant bias in favor of cAMP, with only Chi3-phe1, Ex-ala2-phe1, and Ex-phe1 showing statistically significant changes compared to their His1 counterparts. This may partly relate to the inherently increased imprecision for low efficacy agonists;[43] alternatively, it could imply that relatively high affinity (as is

https://dx.doi.org/10.1021/acsptsci.0c00022
ACS Pharmacol. Transl. Sci. 2020, 3, 345−360

the case for these three Phe1 ligands) is required for a significant degree of bias. The NanoBiT complementation approach provides a means to compare dynamic G protein versus β-arrestin-2 recruitment events without the caveats of adenylate cyclase amplification of cAMP responses or irreversible enzyme complementation in the DiscoverX system. Here, Phe1 ligands were found in all cases to show lower efficacy for both pathways. This reduction, however, appeared more marked for β-arrestin-2 recruitment, suggesting efficacy-driven bias in favor of G_s. Again, the Gly2-containing Phe1 ligands showed the greatest signaling deficit of all, with small magnitude responses even for G_s recruitment (which are, nevertheless, sufficient to produce full cAMP responses in the context of adequate amplification by adenylate cyclase). It should be noted that mini-G protein recruitment responses do not fully recapitulate G protein activation dynamics, which have recently been studied using NanoBRET-based sensors[44] and would be an interesting future investigation for these ligands. The β-arrestin-2 recruitment response of Chi2-phe1 was greater than that of other Phe1 agonists, which was not observed in the DiscoverX assay; this observation remains unexplained. A limitation of our study is that we measured β-arrestin recruitment and did not record putative β-arrestin-mediated signaling events. β-Arrestin-mediated ERK signaling has been proposed to contribute to insulin secretion,[6] although we note GLP-1R-mediated ERK phosphorylation is at least G protein-dependent[5] and that the signaling role of β-arrestins remains controversial.[45]

GLP-1R recycling data from a wide range of His1- and Phe1-containing ligands provided further insights into the relationship between GLP-1RA binding affinity and postendocytic targeting, as highlighted in our earlier study.[15] In the present work, affinity predicted recycling rates for ligands within a pK_i range of approximately 1−100 nM. The fact that some ligands with presumably enhanced proteolytic stability but lower affinity (e.g., Ex-ala2-phe1) were found to recycle faster than those with reduced stability but higher affinity (e.g., GLP-1) argues against intraendosomal peptide degradation being the dominant factor influencing GLP-1R recycling, but this speculation requires experimental verification.

We performed specific studies in the pancreatic beta cell-like INS-1 832/3 model to identify whether the pharmacological properties of the ligands tested here are potentially relevant to biologically important insulin release. Measures from HEK293 cells were generally replicated in the beta cell model, although some differences in the trafficking characteristics were apparent. In particular, endocytosis was faster and more extensive in INS-1 cells, with His1 ligands reaching a peak DERET signal up to twice as fast as in the HEK293 model, and with a less marked suppression of internalization with many Phe1 ligands also observed. While the specific trafficking characteristics of GLP-1R in HEK293 cells are not in themselves physiologically relevant, it raises the possibility of cell-specific differences in GLP-1R trafficking in physiological systems, that is, a form of "tissue bias".[30] It could be speculated that different GLP-1RAs might therefore behave differently in beta cells and anorectic neurons, for example, although further experiments using primary neurons and beta cells would be required to substantiate this. Moreover, there is current interest in using GPCR-targeting peptides to deliver cargo to metabolically important tissues[46−48] and, as such, tissue-specific GLP-1R endocytic characteristics might be relevant to the targeting efficiency for different cell types and organ systems.

As therapeutic GLP-1RAs have now been engineered for prolonged pharmacokinetics allowing weekly administration, we focused the final part of this study on the beta cell effects of sustained agonist exposure. We observed that the acute trafficking responses of each peptide were reasonably predictive of surface GLP-1R levels after prolonged treatment, with fast recycling generally associated with greater detection of surface GLP-1R at the end of the incubation period. The slow internalizing/fast recycling compounds (such as Ex-phe1 and GLP-1-gly2-phe1) had some of the highest levels of GLP-1R remaining at the surface in this assay. Interestingly, in spite of almost complete SNAP-GLP-1R internalization within 30 min of high efficacy His1 agonist stimulation detected using cleavable BG-S-S-probes earlier in this study, the poststimulation labeling approach suggested GLP-1R surface levels remained at least at 30% of those of in vehicle-treated cells despite a prolonged stimulation period at a high agonist dose. This may partly represent GLP-1R recycling during the labeling period but could also represent delivery of newly synthesized or constitutively recycled GLP-1Rs to the cell surface, which would not be detected using the prestimulation labeling approach.

Interestingly, functional readouts in wild-type INS-1 832/3 cells, including homologous desensitization and insulin secretion, did not perfectly recapitulate the pattern of GLP-1R observed with prolonged agonist exposure. One example is the comparison between His1 and Phe1 versions of Ex-ala2 and exendin-4; here, both Phe1 ligands showed clearly reduced homologous desensitization and improved insulin secretion, yet surface GLP-1R levels with Ex-ala2-phe1 were no different to Ex-ala2-his1. Further complexities in the spatiotemporal control of signaling might contribute to this dichotomy. Additionally, differences between the cell systems and receptor species used for trafficking (INS-1 832/3 GLP-1R$^{-/-}$ cells with human SNAP-GLP-1R overexpression) and functional studies (wild-type INS-1 832/3 cells with endogenous rat GLP-1R expression) could be relevant. Insertion of biorthogonal tags, for example, SNAP or Halo, into the endogenous receptor genomic sequence by CRISPR/Cas9[49] may allow these events to be studied without overexpression artifacts and should be used in the future. Fluorescent ligands can also be used to study endogenous GLP-1R dynamics,[24] provided fluorophore bioconjugation to a relatively large number of peptides (as in this study) is feasible and does not interfere with ligand pharmacological properties.

Because of confounding from inherent pharmacokinetic differences between GLP-1- and exendin-4-like peptides, we did not aim to determine if the ligand-specific pharmacological characteristics influence their antihyperglycaemic or anorectic properties *in vivo*. Our previous study with biased exendin-4-derived analogues, however, suggested retention of sensitized GLP-1R at the plasma membrane, for example, with exendin-phe1, enhances antidiabetic effectiveness.[15] We note also that large trials have revealed heterogeneity in clinical outcomes with different GLP-1RAs,[18,19] with one possible explanation being their divergent pharmacology. Fatty acid conjugation to peptides prolongs pharmacokinetics by reducing glomerular filtration through the promotion of reversible binding to albumin; this approach could be taken with the chimeric peptides in the present study to allow them to be evaluated *in vivo*. However, the acyl chain orientation is likely to be

https://dx.doi.org/10.1021/acsptsci.0c00022
ACS Pharmacol. Transl. Sci. 2020, 3, 345−360

influenced by sequence changes in the main peptide helix, potentially affecting both ligand affinity for GLP-1R and albumin,[50] thereby complicating interpretation. Moreover, whether the persistent binding to albumin of the internalized ligand could influence postendocytic sorting via the neonatal Fc receptor (FcRn),[51] one of the top 10% expressed genes in beta cells,[52] is an interesting and open question. A pragmatic way to test whether signal bias can be used to improve existing therapies would be to introduce the Phe1 substitution to the N-termini of established GLP-1RAs such as Liraglutide or Semaglutide.

In summary, this work provides a systematic evaluation of a panel of GLP-1RAs with varying homology to GLP-1 and exendin-4. We identified marked differences in signaling, endocytosis and trafficking characteristics, which may be informative for the development of improved GLP-1RAs for T2D and obesity. As most of our observations are correlative, future work could involve testing some of the ligands described herein in combination with the wide range of mutant GLP-1R constructs that have been published[5,53,54] to gain a better understanding of ligand−receptor interactions important for specific GLP-1R behaviors.

3. METHODS

3.1. Peptides and Reagents. Peptides were obtained from Wuxi Apptec and were at least 90% pure. Homogenous time-resolved fluorescence (HTRF) reagents, including cAMP Dynamic 2 kit, wide-range insulin HTRF kit, SNAP-Lumi4-Tb, and cleavable BG-S-S-Lumi4-Tb, were obtained from Cisbio. PathHunter detection reagents were obtained from DiscoverX. SNAP-Surface-549 and -649 probes were obtained from New England Biolabs. The cleavable BG-S-S-649 probe was a gift from New England Biolabs. Cell culture reagents were obtained from Sigma and Thermo Fisher Scientific.

3.2. Cell Culture. HEK293T cells were maintained in DMEM supplemented with 10% FBS and 1% penicillin/streptomycin. HEK293-SNAP-GLP-1R cells, generated by stable transfection of pSNAP-GLP-1R (Cisbio), previously described in ref 55 were maintained in DMEM supplemented with 10% FBS, 1% penicillin/streptomycin, and 1 mg/mL G418. PathHunter CHO-K1-βarr2-EA-GLP-1R cells were maintained in Ham's F12 medium supplemented with 10% FBS, 1% penicillin/streptomycin, 1 mg/mL G418, and 0.4 mg/mL hygromycin B. CHO-K1-SNAP-GLP-1R cells[55] were maintained in DMEM supplemented with 10% FBS, 10 mM HEPES, 1% nonessential amino acids, 1% penicillin/streptomycin, and 1 mg/mL G418. Wildtype INS-1 832/3 cells (a gift from Prof. Christopher Newgard, Duke University),[31] and INS-1 832/3 cells lacking endogenous GLP-1R after deletion by CRISPR/Cas9 (INS-1 832/3 GLP-1R$^{-/-}$ cells, a gift from Dr Jacqueline Naylor, MedImmune, Astra Zeneca),[56] were maintained in RPMI-1640 with 11 mM glucose, 10 mM HEPES, 2 mM glutamine, 1 mM sodium pyruvate, 50 μM β-mercaptoethanol, 10% FBS, and 1% penicillin/streptomycin. INS-1-SNAP-GLP-1R cells, used for beta cell GLP-1R trafficking assays, were generated from INS-1 832/3 GLP-1R$^{-/-}$ cells by stable transfection of pSNAP-GLP-1R and selection with G418 (1 mg/mL).

3.3. TR-FRET Equilibrium Binding Assays. The binding of test peptides was monitored in competition with the fluorescent agonist exendin-4-FITC, in which the FITC is conjugated to Lys12 of the native exendin-4 sequence.[57] Assays were performed in HEK293-SNAP-GLP-1R cells labeled with SNAP-Lumi4-Tb (40 μM, 30 min, in complete medium) followed by washing and resuspension in HBSS with 0.1% BSA, and supplemented with metabolic inhibitors (20 mM 2-deoxyglucose and 10 mM NaN_3) to maintain GLP-1R at the cell surface during the assay.[58] Labeled cells were placed at 4 °C before addition of a range of concentrations of test peptides prepared in HBSS with 0.1% BSA containing 4 nM exendin-4-FITC. A range of concentrations of exendin-4-FITC was also used to establish K_d by saturation binding analysis for the assay. Cells were then incubated for 24 h at 4 °C before being read by time-resolved Förster resonance energy transfer (TR-FRET) in a Flexstation 3 plate reader (Molecular Devices) with the use of the following settings: λ_{ex} = 335 nm, λ_{em} = 520 and 620 nm, delay = 50 μs, and integration time = 400 μs. Binding was quantified as the ratio of fluorescent signal at 520 nm to that at 620 nm, after subtraction of the ratio obtained in the absence of FITC-ligands. IC_{50} values for test peptides were determined using the "one site−fit K_i" model in Prism 8.0 (GraphPad Software), with the K_d result for exendin-4-FITC obtained using the "one site−specific binding" model for that experiment used to constrain the assay.

3.4. Acute Cyclic AMP Assays. Cells were seeded into white 96-well half area plates and stimulated with the indicated concentration of agonist in serum-free medium. CHO-K1-βarr2-EA-GLP-1R and HEK293-SNAP-GLP-1R cells were treated for 30 min at 37 °C without phosphodiesterase inhibitors. Wild-type INS-1 832/3 cells, after a 6-h preincubation in low glucose (3 mM) complete medium, were stimulated for 10 min at 37 °C with 500 μM 3-isobutyl-1-methylxanthine (IBMX). HTRF detection reagents (cAMP Dynamic 2 kit, Cisbio) were added at the end of the incubation, and the plate was read after a further 60 min incubation by HTRF using a Spectramax i3x plate reader (Molecular Devices).

3.5. PathHunter β-Arrestin Recruitment Assays. CHO-K1-βarr2-EA-GLP-1R cells were seeded into white 96-well half area plates and stimulated for 30 min at 37 °C with the indicated concentration of agonist in serum-free Ham's F12 medium. PathHunter detection reagents were added, and luminescence readings were taken after 60 min at room temperature using a Spectramax i3x plate reader.

3.6. Homologous Desensitization Assay. INS-1 832/3 cells were seeded into 96 well tissue-culture treated plates previously coated with 0.1% poly-D-lysine, in complete medium at 11 mM glucose. Ligands were promptly added without IBMX and cells were incubated for 16 h overnight at 37 °C. The next day, the medium was removed, and cells were washed three times in HBSS. After a 60 min recycling period in complete medium, cells were washed once more, and complete medium containing 500 μM IBMX + GLP-1 (100 nM) was added for 10 min before cell lysis. Lysates were analyzed for cAMP concentration by HTRF as above, and the results were expressed relative to the vehicle pretreatment control cells.

3.7. Insulin Secretion Measurements. Wild-type INS-1 832/3 cells were exposed to a 6-h preincubation in low glucose (3 mM) complete medium before the assay. Cells were seeded in suspension into complete medium with 11 mM glucose ± agonist and incubated for 16 h at 37 °C. Secreted insulin in the supernatant was analyzed by HTRF (Insulin High Range kit, Cisbio) after dilution and normalized to the concentration in glucose-only treated wells.

3.8. NanoBiT Complementation Assays. The GLP-1R-SmBiT plasmid was generated following digestion of GLP-1R-

https://dx.doi.org/10.1021/acsptsci.0c00022
ACS Pharmacol. Transl. Sci. 2020, 3, 345−360

Tango (Addgene plasmid no. 66295, a gift from Bryan Roth), with AgeI and XbaI and ligation of a duplexed SmBiT sequence (SmBiT F: 5′-ccggtggtggatccggcggaggtgtgaccg-gctaccggctgttcgaggagattctgtaat-3′; SmBiT R: 5′-gatctaatgtc-ttagaggagcttgtcggccatcggccagtgtggaggcggcctaggtggt-3′). The assay was performed as previously described.[25] HEK293T cells in 12-well plates were cotransfected with 0.05 μg each of GLP-1R-SmBiT and βarr2-LgBiT plasmid (Promega) plus 0.9 μg of pcDNA3.1, or with 0.5 μg each of GLP-1R-SmBiT and LgBiT-mini-G_s plasmid (a gift from Prof Nevin Lambert, Medical College of Georgia).[27] The assay was performed 24−36 h later. Cells were detached, resuspended in NanoGlo Live Cell Reagent (Promega) with furimazine (1:20 dilution) and seeded into white 96-well half area plates. Baseline luminescence was immediately recorded over 5 min at 37 °C in a Flexstation 3 plate reader, and serially after agonist addition for 30 min.

3.9. Measurement of GLP-1R Internalization by DERET. The assay was performed as previously described.[55] Cells were labeled with SNAP-Lumi4-Tb (40 μM, 30 min, in complete medium), washed, and resuspended in HBSS with 24 μM fluorescein. TR-FRET signals at baseline and serially after agonist addition were recorded at 37 °C using a Flexstation 3 plate reader using the following settings: λ_{ex} = 335 nm, λ_{em} = 520 and 620 nm, delay = 400 μs, and integration time = 1500 μs. Receptor internalization was quantified as the ratio of fluorescent signal at 620 nm to that at 520 nm, after subtraction of individual wavelength signals obtained from wells containing 24 μM fluorescein only.

3.10. TR-FRET GLP-1R Recycling Assay. The method was adapted from a previous description,[25] with the main change being the use of LUXendin645[24] as the TR-FRET acceptor to improve signal-to-noise ratio. Adherent CHO-K1-SNAP-GLP-1R cells in 96-well half area tissue culture-treated plates were labeled with BG-S-S-Lumi4-Tb (40 μM, 30 min in complete medium), followed by washing. Agonist treatments were applied in serum-free medium for 30 min at 37 °C. The plate was then placed on ice, washed with cold HBSS followed by a 5 min application of cold Mesna (100 mM in alkaline TNE buffer) to cleave Lumi4-Tb from receptors remaining at the cell surface. After further washing in the cold, warm HBSS containing 10 nM LUXendin645 was then added, and TR-FRET was serially monitored at 616 and 665 nm. Reappearance at the plasma membrane of Lumi4-Tb-labeled SNAP-GLP-1R is thus determined as an increase in TR-FRET, expressed ratiometrically as signal intensity at 665 nm divided by that at 616 nm.

3.11. Imaging of Receptor Redistribution. Cells seeded overnight on coverslips were labeled for 30 min at 37 °C with SNAP-Surface 549 (1 μM) to label surface SNAP-GLP-1Rs. After the cells were washed, treatments were applied for 30 min at 37 °C. Where indicated, cells were washed in HBSS twice and incubated in complete medium for 1 h to allow GLP-1R recycling. A further wash in HBSS followed, and the surface receptor was labeled with LUXendin645 (100 nM) for 5 min. Cells were fixed with 2% paraformaldehyde for 20 min at room temperature. Coverslips were mounted with Diamond Prolong antifade (Thermo Fisher) with DAPI and imaged using a modular microscope platform from Cairn Research incorporating a Nikon Ti2E, LED light source (CoolLED) and a 0.95 numerical aperture 40× air objective, or 1.45 numerical aperture 100× oil immersion objective. Where indicated, Z-stacks were acquired and deconvolved using Huygens software (SVI). Image galleries were generated using Fiji.

3.12. High Content Microscopy Internalization/Recycling Assay. Cells were seeded into poly-D-lysine-coated, black 96-well plates to promote attachment and avoid cell loss during the wash steps. On the day of the assay, labeling was performed with BG-S-S-649 (1 μM), a surface-labeling SNAP-tag probe that, like BG-S-S-Lumi4-Tb, can be released on application of reducing agents such as Mesna.[10,32] After the cells were washed, treatments were applied for 30 min at 37 °C in complete medium. The ligand was removed, and cells were washed with cold HBSS, and placed on ice for subsequent steps. Mesna (100 mM in alkaline TNE buffer, pH 8.6) or alkaline TNE without Mesna was applied for 5 min, and then washed with HBSS. Microplate imaging was performed immediately without fixation, using the microscope system described in section 3.11 fitted with a 20× phase contrast objective, assisted by custom-written high content analysis software[59] implemented in Micro-Manager.[60] A minimum of six images per well was acquired for both epifluorescence and transmitted phase contrast. On completion of imaging, HBSS was removed and replaced with fresh complete medium and the receptor was allowed to recycle for 60 min at 37 °C, followed by a second Mesna application to remove any receptor that had recycled to the membrane, and the plate was reimaged as above. Internalized SNAP-GLP-1R was quantified at both time points as follows using Fiji: (1) phase contrast images were processed using PHANTAST[61] to segment cell-containing regions from background; (2) illumination correction of fluorescence images was performed using BaSiC;[62] (3) fluorescence intensity was quantified for cell-containing regions. Agonist-mediated internalization was determined as the mean signal for each condition normalized to signal from wells not treated with Mesna, after first subtracting nonspecific fluorescence determined from wells treated with Mesna but no agonist. The percentage reduction in the residual internalized receptor after the second Mesna treatment was considered to represent the recycled receptor. Recycling was then expressed as a percentage relative to the amount of receptor originally internalized in the same well.

3.13. Post-Treatment Receptor Labeling Assay. INS-1-SNAP-GLP-1R cells were seeded into poly-D-lysine-coated, black 96-well plates, and treatments were promptly applied. Wild-type INS-1 832/3 (without SNAP-tag) were used as a control to account for any contribution of nonspecific labeling. After a 16 h overnight incubation, cells were washed three times in HBSS and labeled for 1 h at 37 °C with 1 μM SNAP-Surface-649, before washing and imaging. Imaging settings and cell segmentation were performed as described in section 3.12. Mean signal intensity from wild-type INS-1 832/3 cells was subtracted, allowing the surface SNAP-GLP-1R expression after agonist treatment to be expressed relative to vehicle-treated INS-1 832/3 SNAP-GLP-1R cells.

3.14. Data Analysis and Statistics. Quantitative data were analyzed using Prism 8.0. One biological replicate was treated as the average of technical replicates from an independently performed experiment. Intensity quantification from imaging data was performed on full depth 16-bit data after illumination correction; images are displayed with reduced dynamic range to highlight dim structures, with the same brightness and contrast settings consistently applied across matched images. Binding affinity calculations are described in section 3.3. A 3-parameter logistic fitting was

https://dx.doi.org/10.1021/acsptsci.0c00022
ACS Pharmacol. Transl. Sci. 2020, 3, 345−360

performed for concentration response analyses with constraints imposed as described in the table legends. For bias calculations, to reduce the contribution of interassay variability and to avoid artifactual bias resulting from different activation kinetics of each pathway,[63] cAMP and β-arrestin-2 assays were performed concurrently, with the same incubation time of 30 min; bias was determined by calculating transduction coefficients;[22,64] here, due to the matched design of our experiments, we calculated $\Delta\Delta\log(\tau/K_A)$ on a per-assay basis by normalizing the $\log(\tau/K_A)$ for each ligand to the reference ligand (GLP-1) and then to the reference pathway (β-arrestin-2). Principal component analysis was performed using ClustVis[65] using the "SVD with imputation" method with unit variance scaling applied. ANOVA and t test approaches were used for statistical comparisons. In experiments with a matched design, randomized block one-way ANOVA was used to compare treatments, with specific posthoc tests indicated in the figure legends. Statistical significance was inferred when $p < 0.05$. Data are represented as mean ± SEM throughout, with individual experimental replicates shown where possible.

■ ASSOCIATED CONTENT

Supporting Information

. The Supporting Information is available free of charge at https://pubs.acs.org/doi/10.1021/acsptsci.0c00022.

SNAP-GLP-1R internalization rates for each ligand in HEK293 and INS-1 832/3 cell; additional binding, signaling, and trafficking data for chimeric GLP-1R ligands; Phe1-substituted ligand evaluation; effects in beta cells (PDF)

■ AUTHOR INFORMATION

Corresponding Authors

Ben Jones − *Section of Endocrinology and Investigative Medicine, Imperial College London, London W12 0NN, United Kingdom;* orcid.org/0000-0003-0461-2584; Email: ben.jones@imperial.ac.uk

Alejandra Tomas − *Section of Cell Biology and Functional Genomics, Imperial College London, London SW7 2AZ, United Kingdom*; Email: a.tomas-catala@imperial.ac.uk

Authors

Zijian Fang − *Section of Endocrinology and Investigative Medicine, Imperial College London, London W12 0NN, United Kingdom*

Shiqian Chen − *Section of Endocrinology and Investigative Medicine, Imperial College London, London W12 0NN, United Kingdom*

Philip Pickford − *Section of Endocrinology and Investigative Medicine, Imperial College London, London W12 0NN, United Kingdom*

Johannes Broichhagen − *Department Chemical Biology, Leibniz-Forschungsinstitut für Molekulare Pharmakologie (FMP), Berlin 13125, Germany*

David J. Hodson − *Institute of Metabolism and Systems Research (IMSR), and Centre of Membrane Proteins and Receptors (COMPARE), University of Birmingham, Birmingham B15 2TT, United Kingdom; Centre for Endocrinology, Diabetes and Metabolism, Birmingham Health Partners, Birmingham B15 2TT, United Kingdom;* orcid.org/0000-0002-8641-8568

Ivan R. Corrêa, Jr. − *New England Biolabs, Ipswich, Massachusetts 01938, United States;* orcid.org/0000-0002-3169-6878

Sunil Kumar − *Department of Physics, Imperial College London, London SW7 2BX, United Kingdom*

Frederik Görlitz − *Department of Physics, Imperial College London, London SW7 2BX, United Kingdom*

Chris Dunsby − *Department of Physics, Imperial College London, London SW7 2BX, United Kingdom*

Paul M. W. French − *Department of Physics, Imperial College London, London SW7 2BX, United Kingdom*

Guy A. Rutter − *Section of Cell Biology and Functional Genomics, Imperial College London, London SW7 2AZ, United Kingdom*

Tricia Tan − *Section of Endocrinology and Investigative Medicine, Imperial College London, London W12 0NN, United Kingdom*

Stephen R. Bloom − *Section of Endocrinology and Investigative Medicine, Imperial College London, London W12 0NN, United Kingdom*

Complete contact information is available at: https://pubs.acs.org/10.1021/acsptsci.0c00022

Author Contributions

[▽]These authors contributed equally. Z.F., S.C., P.P., B.J., and A.T. designed the study and performed experiments. J.B., D.J.H., and I.R.C. provided novel reagents. S.K., F.G., C.D., and P.F. developed software for high content image analysis. B.J., A.T., S.R.B., G.A.R., and T.T. acquired core funding for this project. B.J. and A.T. wrote the manuscript. All authors reviewed and approved the manuscript.

Notes

The authors declare the following competing financial interest(s): G.A.R. is a consultant for Sun Pharmaceuticals and has received grant funding from Sun Pharmaceuticals and Les Laboratoires Servier. B.J. and A.T. have received grant funding from Sun Pharmaceuticals.

■ ACKNOWLEDGMENTS

This work was funded by an MRC project grant to B.J., A.T., S.R.B., and G.A.R and supported by the EFSD/Boehringer Ingelheim European Research Programme on "Multi-System Challenges in Diabetes" to B.J. and A.T. The Section of Endocrinology and Investigative Medicine is funded by grants from the MRC, BBSRC, NIHR, an Integrative Mammalian Biology (IMB) Capacity Building Award, an FP7-HEALTH-2009-241592 EuroCHIP grant and is supported by the NIHR Biomedical Research Centre Funding Scheme. The views expressed are those of the author(s) and not necessarily those of the funder. B.J. was also supported by the Academy of Medical Sciences, Society for Endocrinology and an EPSRC capital award. D.J.H. was supported by MRC (MR/N00275X/1 and MR/S025618/1) and Diabetes UK (17/0005681) project grants. This project has received funding from the European Research Council (ERC) under the European Union's Horizon 2020 research and innovation programme (Starting Grant 715884 to D.J.H.). G.A.R. was supported by a Wellcome Trust Investigator Award (212625/Z/18/Z), MRC Programme grants (MR/R022259/1, MR/J0003042/1, MR/L020149/1), Experimental Challenge grant (DIVA, MR/L02036X/1), MRC (MR/N00275X/1), and Diabetes UK (BDA/11/0004210, BDA/15/0005275, BDA 16/0005485)

grants. This project has received funding from the European Union's Horizon 2020 research and innovation programme via the Innovative Medicines Initiative 2 Joint Undertaking under Grant Agreement No. 115881 (RHAPSODY) to G.A.R.

REFERENCES

(1) Ogurtsova, K., da Rocha Fernandes, J. D., Huang, Y., Linnenkamp, U., Guariguata, L., Cho, N. H., Cavan, D., Shaw, J. E., and Makaroff, L. E. (2017) IDF Diabetes Atlas: Global estimates for the prevalence of diabetes for 2015 and 2040. *Diabetes Res. Clin. Pract. 128*, 40−50.

(2) Finkelstein, E. A., Khavjou, O. A., Thompson, H., Trogdon, J. G., Pan, L., Sherry, B., and Dietz, W. (2012) Obesity and severe obesity forecasts through 2030. *Am. J. Prev. Med. 42*, 563−570.

(3) Andersen, A., Lund, A., Knop, F. K., and Vilsbøll, T. (2018) Glucagon-like peptide 1 in health and disease. *Nat. Rev. Endocrinol. 14*, 390−403.

(4) de Graaf, C., Donnelly, D., Wootten, D., Lau, J., Sexton, P. M., Miller, L. J., Ahn, J.-M., Liao, J., Fletcher, M. M., Yang, D., Brown, A. J. H., Zhou, C., Deng, J., and Wang, M.-W. (2016) Glucagon-Like Peptide-1 and Its Class B G Protein-Coupled Receptors: A Long March to Therapeutic Successes. *Pharmacol. Rev. 68*, 954−1013.

(5) Wootten, D., Reynolds, C. A., Smith, K. J., Mobarec, J. C., Koole, C., Savage, E. E., Pabreja, K., Simms, J., Sridhar, R., Furness, S. G. B., Liu, M., Thompson, P. E., Miller, L. J., Christopoulos, A., and Sexton, P. M. (2016) The Extracellular Surface of the GLP-1 Receptor Is a Molecular Trigger for Biased Agonism. *Cell 165*, 1632−1643.

(6) Sonoda, N., Imamura, T., Yoshizaki, T., Babendure, J. L., Lu, J.-C., and Olefsky, J. M. (2008) Beta-Arrestin-1 mediates glucagon-like peptide-1 signaling to insulin secretion in cultured pancreatic beta cells. *Proc. Natl. Acad. Sci. U. S. A. 105*, 6614−6619.

(7) Jones, B., Bloom, S. R., Buenaventura, T., Tomas, A., and Rutter, G. A. (2018) Control of insulin secretion by GLP-1. *Peptides 100*, 75−84.

(8) Kenakin, T. (2018) Is the Quest for Signaling Bias Worth the Effort? *Mol. Pharmacol. 93*, 266−269.

(9) Kuna, R. S., Girada, S. B., Asalla, S., Vallentyne, J., Maddika, S., Patterson, J. T., Smiley, D. L., Dimarchi, R. D., and Mitra, P. (2013) Glucagon-like peptide-1 receptor-mediated endosomal cAMP generation promotes glucose-stimulated insulin secretion in pancreatic β-cells. *Am. J. Physiol Endocrinol Metab 305*, E161−70.

(10) Buenaventura, T., Kanda, N., Douzenis, P. C., Jones, B., Bloom, S. R., Chabosseau, P., Corrêa, I. R., Bosco, D., Piemonti, L., Marchetti, P., Johnson, P. R., Shapiro, A. M. J., Rutter, G. A., and Tomas, A. (2018) A Targeted RNAi Screen Identifies Endocytic Trafficking Factors That Control GLP-1 Receptor Signaling in Pancreatic β-Cells. *Diabetes 67*, 385−399.

(11) Fletcher, M. M., Halls, M. L., Zhao, P., Clydesdale, L., Christopoulos, A., Sexton, P. M., and Wootten, D. (2018) Glucagon-like peptide-1 receptor internalisation controls spatiotemporal signalling mediated by biased agonists. *Biochem. Pharmacol. 156*, 406−419.

(12) Edwards, C. M., Stanley, S. A., Davis, R., Brynes, A. E., Frost, G. S., Seal, L. J., Ghatei, M. A., and Bloom, S. R. (2001) Exendin-4 reduces fasting and postprandial glucose and decreases energy intake in healthy volunteers. *Am. J. Physiol Endocrinol Metab 281*, E155−61.

(13) Kolterman, O. G., Buse, J. B., Fineman, M. S., Gaines, E., Heintz, S., Bicsak, T. A., Taylor, K., Kim, D., Aisporna, M., Wang, Y., and Baron, A. D. (2003) Synthetic exendin-4 (exenatide) significantly reduces postprandial and fasting plasma glucose in subjects with type 2 diabetes. *J. Clin. Endocrinol. Metab. 88*, 3082−3089.

(14) Zhang, H., Sturchler, E., Zhu, J., Nieto, A., Cistrone, P. A., Xie, J., He, L., Yea, K., Jones, T., Turn, R., Di Stefano, P. S., Griffin, P. R., Dawson, P. E., McDonald, P. H., and Lerner, R. A. (2015) Autocrine selection of a GLP-1R G-protein biased agonist with potent antidiabetic effects. *Nat. Commun. 6*, 8918.

(15) Jones, B., Buenaventura, T., Kanda, N., Chabosseau, P., Owen, B. M., Scott, R., Goldin, R., Angkathunyakul, N., Corrêa, I. R., Bosco, D., Johnson, P. R., Piemonti, L., Marchetti, P., Shapiro, A. M. J., Cochran, B. J., Hanyaloglu, A. C., Inoue, A., Tan, T., Rutter, G. A., Tomas, A., and Bloom, S. R. (2018) Targeting GLP-1 receptor trafficking to improve agonist efficacy. *Nat. Commun. 9*, 1602.

(16) Fremaux, J., Venin, C., Mauran, L., Zimmer, R., Koensgen, F., Rognan, D., Bitsi, S., Lucey, M. A., Jones, B., Tomas, A., Guichard, G., and Goudreau, S. R. (2019) Ureidopeptide GLP-1 analogues with prolonged activity in vivo via signal bias and altered receptor trafficking. *Chem. Sci. 10*, 9872−9879.

(17) Andersen, A., Lund, A., Knop, F. K., and Vilsbøll, T. (2018) Glucagon-like peptide 1 in health and disease. *Nat. Rev. Endocrinol. 14*, 390−403.

(18) Holman, R. R., Bethel, M. A., Mentz, R. J., Thompson, V. P., Lokhnygina, Y., Buse, J. B., Chan, J. C., Choi, J., Gustavson, S. M., Iqbal, N., Maggioni, A. P., Marso, S. P., Ohman, P., Pagidipati, N. J., Poulter, N., Ramachandran, A., Zinman, B., and Hernandez, A. F. (2017) Effects of Once-Weekly Exenatide on Cardiovascular Outcomes in Type 2 Diabetes. *N. Engl. J. Med. 377*, 1228−1239.

(19) Marso, S. P., Bain, S. C., Consoli, A., Eliaschewitz, F. G., Jodar, E., Leiter, L. A., Lingvay, I., Rosenstock, J., Seufert, J., Warren, M. L., Woo, V., Hansen, O., Holst, A. G., Pettersson, J., and Vilsbøll, T. (2016) Semaglutide and Cardiovascular Outcomes in Patients with Type 2 Diabetes. *N. Engl. J. Med. 375*, 1834−1844.

(20) Montrose-Rafizadeh, C., Yang, H., Rodgers, B. D., Beday, A., Pritchette, L. A., and Eng, J. (1997) High potency antagonists of the pancreatic glucagon-like peptide-1 receptor. *J. Biol. Chem. 272*, 21201−21206.

(21) Jorgensen, R., Kubale, V., Vrecl, M., Schwartz, T. W., and Elling, C. E. (2007) Oxyntomodulin differentially affects glucagon-like peptide-1 receptor beta-arrestin recruitment and signaling through Galpha(s). *J. Pharmacol. Exp. Ther. 322*, 148−154.

(22) van der Westhuizen, E. T., Breton, B., Christopoulos, A., and Bouvier, M. (2014) Quantification of ligand bias for clinically relevant β2-adrenergic receptor ligands: implications for drug taxonomy. *Mol. Pharmacol. 85*, 492−509.

(23) Levoye, A., Zwier, J. M., Jaracz-Ros, A., Klipfel, L., Cottet, M., Maurel, D., Bdioui, S., Balabanian, K., Prézeau, L., Trinquet, E., Durroux, T., and Bachelerie, F. (2015) A Broad G Protein-Coupled Receptor Internalization Assay that Combines SNAP-Tag Labeling, Diffusion-Enhanced Resonance Energy Transfer, and a Highly Emissive Terbium Cryptate. *Front. Endocrinol. (Lausanne, Switz.) 6*, 167.

(24) Ast, J., Arvaniti, A., Fine, N. H. F., Nasteska, D., Ashford, F. B., Stamataki, Z., Koszegi, Z., Bacon, A., Jones, B. J., Lucey, M. A., Sasaki, S., Brierley, D. I., Hastoy, B., Tomas, A., D'Agostino, G., Reimann, F., Lynn, F. C., Reissaus, C. A., Linnemann, A. K., D'Este, E., Calebiro, D., Trapp, S., Johnsson, K., Podewin, T., Broichhagen, J., and Hodson, D. J. (2020) Super-resolution microscopy compatible fluorescent probes reveal endogenous glucagon-like peptide-1 receptor distribution and dynamics. *Nat. Commun. 11*, 467.

(25) Pickford, P., Lucey, M., Fang, Z., Bitsi, S., Broichhagen, J., Hodson, D. J., Minnion, J., Rutter, G. A., Bloom, S. R., Tomas, A., and Jones, B.. (2019) Differences in signalling, trafficking and glucoregulatory properties of glucagon-like peptide-1 receptor agonists exendin-4 and lixisenatide. *Biorxiv* October 16, 2019. DOI: 10.1101/803833.

(26) Dixon, A. S., Schwinn, M. K., Hall, M. P., Zimmerman, K., Otto, P., Lubben, T. H., Butler, B. L., Binkowski, B. F., Machleidt, T., Kirkland, T. A., Wood, M. G., Eggers, C. T., Encell, L. P., and Wood, K. V. (2016) NanoLuc Complementation Reporter Optimized for Accurate Measurement of Protein Interactions in Cells. *ACS Chem. Biol. 11*, 400−408.

(27) Wan, Q., Okashah, N., Inoue, A., Nehmé, R., Carpenter, B., Tate, C. G., and Lambert, N. A. (2018) Mini G protein probes for active G protein-coupled receptors (GPCRs) in live cells. *J. Biol. Chem. 293*, 7466−7473.

(28) Kenakin, T. (2016) The mass action equation in pharmacology. *Br. J. Clin. Pharmacol. 81*, 41−51.

(29) Thompson, G. L., Lane, J. R., Coudrat, T., Sexton, P. M., Christopoulos, A., and Canals, M. (2015) Biased Agonism of

Endogenous Opioid Peptides at the μ-Opioid Receptor. *Mol. Pharmacol. 88*, 335−346.
(30) Steen, A., Larsen, O., Thiele, S., and Rosenkilde, M. M. (2014) Biased and g protein-independent signaling of chemokine receptors. *Front. Immunol. 5*, 277.
(31) Hohmeier, H. E., Mulder, H., Chen, G., Henkel-Rieger, R., Prentki, M., and Newgard, C. B. (2000) Isolation of INS-1-derived cell lines with robust ATP-sensitive K+ channel-dependent and -independent glucose-stimulated insulin secretion. *Diabetes 49*, 424−430.
(32) Cole, N. B., and Donaldson, J. G. (2012) Releasable SNAP-tag probes for studying endocytosis and recycling. *ACS Chem. Biol. 7*, 464−469.
(33) Görlitz, F., Kelly, D. J., Warren, S. C., Alibhai, D., West, L., Kumar, S., Alexandrov, Y., Munro, I., Garcia, E., McGinty, J., Talbot, C., Serwa, R. A., Thinon, E., da Paola, V., Murray, E. J., Stuhmeier, F., Neil, M. A. A., Tate, E. W., Dunsby, C., and French, P. M. W. (2017) Open Source High Content Analysis Utilizing Automated Fluorescence Lifetime Imaging Microscopy. *J. Visualized Exp.*, No. e55119.
(34) Lee, J. G., Ryu, J. H., Kim, S.-M., Park, M.-Y., Kim, S.-H., Shin, Y. G., Sohn, J.-W., Kim, H. H., Park, Z.-Y., Seong, J. Y., and Kim, J. I. (2018) Replacement of the C-terminal Trp-cage of exendin-4 with a fatty acid improves therapeutic utility. *Biochem. Pharmacol. 151*, 59−68.
(35) Koole, C., Reynolds, C. A., Mobarec, J. C., Hick, C., Sexton, P. M., and Sakmar, T. P. (2017) Genetically encoded photocross-linkers determine the biological binding site of exendin-4 peptide in the N-terminal domain of the intact human glucagon-like peptide-1 receptor (GLP-1R). *J. Biol. Chem. 292*, 7131−7144.
(36) Song, X., Yu, Y., Shen, C., Wang, Y., and Wang, N. (2020) Dimerization/oligomerization of the extracellular domain of the GLP-1 receptor and the negative cooperativity in its ligand binding revealed by the improved NanoBiT. *FASEB J. 277*, 16718.
(37) Harikumar, K. G., Wootten, D., Pinon, D. I., Koole, C., Ball, A. M., Furness, S. G. B., Graham, B., Dong, M., Christopoulos, A., Miller, L. J., and Sexton, P. M. (2012) Glucagon-like peptide-1 receptor dimerization differentially regulates agonist signaling but does not affect small molecule allostery. *Proc. Natl. Acad. Sci. U. S. A. 109*, 18607−18612.
(38) Runge, S., Thøgersen, H., Madsen, K., Lau, J., and Rudolph, R. (2008) Crystal structure of the ligand-bound glucagon-like peptide-1 receptor extracellular domain. *J. Biol. Chem. 283*, 11340−11347.
(39) Song, G., Yang, D., Wang, Y., de Graaf, C., Zhou, Q., Jiang, S., Liu, K., Cai, X., Dai, A., Lin, G., Liu, D., Wu, F., Wu, Y., Zhao, S., Ye, L., Han, G. W., Lau, J., Wu, B., Hanson, M. A., Liu, Z.-J., Wang, M.-W., and Stevens, R. C. (2017) Human GLP-1 receptor transmembrane domain structure in complex with allosteric modulators. *Nature 546*, 312−315.
(40) Roed, S. N., Wismann, P., Underwood, C. R., Kulahin, N., Iversen, H., Cappelen, K. A., Schäffer, L., Lehtonen, J., Hecksher-Soerensen, J., Secher, A., Mathiesen, J. M., Bräuner-Osborne, H., Whistler, J. L., Knudsen, S. M., and Waldhoer, M. (2014) Real-time trafficking and signaling of the glucagon-like peptide-1 receptor. *Mol. Cell. Endocrinol. 382*, 938−949.
(41) Willars, G. B., and Lu, J. (2019) Endothelin-converting enzyme-1 regulates glucagon-like peptide-1 receptor signalling and resensitisation. *Biochem. J. 476*, 513−533.
(42) Hupe-Sodmann, K., McGregor, G. P., Bridenbaugh, R., Göke, R., Göke, B., Thole, H., Zimmermann, B., and Voigt, K. (1995) Characterisation of the processing by human neutral endopeptidase 24.11 of GLP-1(7−36) amide and comparison of the substrate specificity of the enzyme for other glucagon-like peptides. *Regul. Pept. 58*, 149−156.
(43) Stahl, E. L., Zhou, L., Ehlert, F. J., and Bohn, L. M. (2015) A novel method for analyzing extremely biased agonism at G protein-coupled receptors. *Mol. Pharmacol. 87*, 866−877.
(44) Inoue, A., Raimondi, F., Kadji, F. M. N., Singh, G., Kishi, T., Uwamizu, A., Ono, Y., Shinjo, Y., Ishida, S., Arang, N., Kawakami, K., Gutkind, J. S., Aoki, J., and Russell, R. B. (2019) Illuminating G-Protein-Coupling Selectivity of GPCRs. *Cell 177*, 1933.
(45) Grundmann, M., Merten, N., Malfacini, D., Inoue, A., Preis, P., Simon, K., Rüttiger, N., Ziegler, N., Benkel, T., Schmitt, N. K., Ishida, S., Müller, I., Reher, R., Kawakami, K., Inoue, A., Rick, U., Kühl, T., Imhof, D., Aoki, J., König, G. M., Hoffmann, C., Gomeza, J., Wess, J., and Kostenis, E. (2018) Lack of beta-arrestin signaling in the absence of active G proteins. *Nat. Commun. 9*, 341.
(46) Tiano, J. P., Tate, C. R., Yang, B. S., DiMarchi, R., and Mauvais-Jarvis, F. (2015) Effect of targeted estrogen delivery using glucagon-like peptide-1 on insulin secretion, insulin sensitivity and glucose homeostasis. *Sci. Rep. 5*, 10211−8.
(47) Quarta, C., Clemmensen, C., Zhu, Z., Yang, B., Joseph, S. S., Lutter, D., Yi, C.-X., Graf, E., García-Cáceres, C., Legutko, B., Fischer, K., Brommage, R., Zizzari, P., Franklin, B. S., Krueger, M., Koch, M., Vettorazzi, S., Li, P., Hofmann, S. M., Bakhti, M., Bastidas-Ponce, A., Lickert, H., Strom, T. M., Gailus-Durner, V., Bechmann, I., Perez-Tilve, D., Tuckermann, J., Hrabé de Angelis, M., Sandoval, D., Cota, D., Latz, E., Seeley, R. J., Müller, T. D., Dimarchi, R. D., Finan, B., and Tschöp, M. H. (2017) Molecular Integration of Incretin and Glucocorticoid Action Reverses Immunometabolic Dysfunction and Obesity. *Cell Metab. 26*, 620−632.e6.
(48) Ämmälä, C., Drury, W. J., Knerr, L., Ahlstedt, I., Stillemark-Billton, P., Wennberg-Huldt, C., Andersson, E.-M., Valeur, E., Jansson-Löfmark, R., Janzén, D., Sundström, L., Meuller, J., Claesson, J., Andersson, P., Johansson, C., Lee, R. G., Prakash, T. P., Seth, P. P., Monia, B. P., and Andersson, S. (2018) Targeted delivery of antisense oligonucleotides to pancreatic β-cells. *Sci. Adv. 4*, No. eaat3386.
(49) White, C. W., Johnstone, E. K. M., See, H. B., and Pfleger, K. D. G. (2019) NanoBRET ligand binding at a GPCR under endogenous promotion facilitated by CRISPR/Cas9 genome editing. *Cell. Signalling 54*, 27−34.
(50) Lau, J., Bloch, P., Schäffer, L., Pettersson, I., Spetzler, J., Kofoed, J., Madsen, K., Knudsen, L. B., McGuire, J., Steensgaard, D. B., Strauss, H. M., Gram, D. X., Knudsen, S. M., Nielsen, F. S., Thygesen, P., Reedtz-Runge, S., and Kruse, T. (2015) Discovery of the Once-Weekly Glucagon-Like Peptide-1 (GLP-1) Analogue Semaglutide. *J. Med. Chem. 58*, 7370−7380.
(51) Knudsen, L. B., and Lau, J. (2019) The Discovery and Development of Liraglutide and Semaglutide. *Front. Endocrinol. (Lausanne, Switz.) 10*, 155.
(52) Segerstolpe, Å., Palasantza, A., Eliasson, P., Andersson, E.-M., Andréasson, A.-C., Sun, X., Picelli, S., Sabirsh, A., Clausen, M., Bjursell, M. K., Smith, D. M., Kasper, M., Ämmälä, C., and Sandberg, R. (2016) Single-Cell Transcriptome Profiling of Human Pancreatic Islets in Health and Type 2 Diabetes. *Cell Metab. 24*, 593−607.
(53) Wootten, D., Savage, E. E., Willard, F. S., Bueno, A. B., Sloop, K. W., Christopoulos, A., and Sexton, P. M. (2013) Differential activation and modulation of the glucagon-like peptide-1 receptor by small molecule ligands. *Mol. Pharmacol. 83*, 822−834.
(54) Wootten, D., Reynolds, C. A., Koole, C., Smith, K. J., Mobarec, J. C., Simms, J., Quon, T., Coudrat, T., Furness, S. G. B., Miller, L. J., Christopoulos, A., and Sexton, P. M. (2016) A Hydrogen-Bonded Polar Network in the Core of the Glucagon-Like Peptide-1 Receptor Is a Fulcrum for Biased Agonism: Lessons from Class B Crystal Structures. *Mol. Pharmacol. 89*, 335−347.
(55) Buenaventura, T., Bitsi, S., Laughlin, W. E., Burgoyne, T., Lyu, Z., Oqua, A. I., Norman, H., McGlone, E. R., Klymchenko, A. S., Corrêa, I. R., Walker, A., Inoue, A., Hanyaloglu, A., Grimes, J., Koszegi, Z., Calebiro, D., Rutter, G. A., Bloom, S. R., Jones, B., Tomas, A., and Titchenell, P. (2019) Agonist-induced membrane nanodomain clustering drives GLP-1 receptor responses in pancreatic beta cells. *PLoS Biol. 17*, No. e3000097.
(56) Naylor, J., Suckow, A. T., Seth, A., Baker, D. J., Sermadiras, I., Ravn, P., Howes, R., Li, J., Snaith, M. R., Coghlan, M. P., and Hornigold, D. C. (2016) Use of CRISPR/Cas-9 engineered INS-1 pancreatic beta cells to define the pharmacology of dual GIPR/GLP-1R agonists. *Biochem. J. 473*, 2881−2891.

https://dx.doi.org/10.1021/acsptsci.0c00022
ACS Pharmacol. Transl. Sci. 2020, 3, 345−360

(57) Hodson, D. J., Mitchell, R. K., Bellomo, E. A., Sun, G., Vinet, L., Meda, P., Li, D., Li, W.-H., Bugliani, M., Marchetti, P., Bosco, D., Piemonti, L., Johnson, P., Hughes, S. J., and Rutter, G. A. (2013) Lipotoxicity disrupts incretin-regulated human β cell connectivity. *J. Clin. Invest. 123*, 4182−4194.
(58) Widmann, C., Dolci, W., and Thorens, B. (1995) Agonist-induced internalization and recycling of the glucagon-like peptide-1 receptor in transfected fibroblasts and in insulinomas. *Biochem. J. 310* (Pt 1), 203−214.
(59) High Content Analysis. https://www.imperial.ac.uk/photonics/research/biophotonics/instruments--software/high-content-analysis/ (accessed March 1, 2020).
(60) Edelstein, A., Amodaj, N., Hoover, K., Vale, R., and Stuurman, N. (2010) Computer control of microscopes using μManager. *Curr. Protoc Mol. Biol. Chapter 14*, No. 14.20, DOI: 10.1002/0471142727.mb1420s92.
(61) Jaccard, N., Griffin, L. D., Keser, A., Macown, R. J., Super, A., Veraitch, F. S., and Szita, N. (2014) Automated method for the rapid and precise estimation of adherent cell culture characteristics from phase contrast microscopy images. *Biotechnol. Bioeng. 111*, 504−517.
(62) Peng, T., Thorn, K., Schroeder, T., Wang, L., Theis, F. J., Marr, C., and Navab, N. (2017) A BaSiC tool for background and shading correction of optical microscopy images. *Nat. Commun. 8*, 14836−7.
(63) Klein Herenbrink, C., Sykes, D. A., Donthamsetti, P., Canals, M., Coudrat, T., Shonberg, J., Scammells, P. J., Capuano, B., Sexton, P. M., Charlton, S. J., Javitch, J. A., Christopoulos, A., and Lane, J. R. (2016) The role of kinetic context in apparent biased agonism at GPCRs. *Nat. Commun. 7*, 10842.
(64) Kenakin, T., Watson, C., Muniz-Medina, V., Christopoulos, A., and Novick, S. (2012) A simple method for quantifying functional selectivity and agonist bias. *ACS Chem. Neurosci. 3*, 193−203.
(65) Metsalu, T., and Vilo, J. (2015) ClustVis: a web tool for visualizing clustering of multivariate data using Principal Component Analysis and heatmap. *Nucleic Acids Res. 43*, W566−70.

https://dx.doi.org/10.1021/acsptsci.0c00022
ACS Pharmacol. Transl. Sci. 2020, 3, 345−360